SYNTHESIS OF A MODEL LIPID AND OBSERVATION OF BEHAVIOUR OF MODEL LIPOSOMES BY ELECTROPHORESIS

By

XU CHUN SONG

B.Sc., University of Science and Technology of China
Hefei, Anhui, P.R.China, 1986

A THESIS SUBMITTED IN PARTIAL FULFILLMENT OF

THE REQUIREMENTS FOR THE DEGREE OF

MASTER OF SCIENCE

in

THE FACULTY OF GRADUATE STUDIES

DEPARTMENT OF CHEMISTRY

We accept this thesis as conforming

to the required standard

THE UNIVERSITY OF BRITISH COLUMBIA

April 1994

In presenting this thesis in partial fulfilment of the requirements for an advanced degree at the University of British Columbia, I agree that the Library shall make it freely available for reference and study. I further agree that permission for extensive copying of this thesis for scholarly purposes may be granted by the head of my department or by his or her representatives. It is understood that copying or publication of this thesis for financial gain shall not be allowed without my written permission.

(Signature)

Department of CHEMISTRY

The University of British Columbia
Vancouver, Canada

Date Apr. 28, 1994

DE-6 (2/88)

ABSTRACT

A model lipid consisting of a cholesterol base, tetraethoxy- spacer and glucuronic acid head group was synthesized. First, the head group was prepared by acetylation and esterification of glucuronolactone to produce methyl (1,2,3,4-tetra-O- acetyl-β-D-glucopyran)uronate (1) which was then brominated to produce methyl (2,3,4-tri-O-acetyl-α-D-glucopyranosyl bromide)uronate (2). The combination of the cholesterol part and tetra-ethoxy chain was made by reacting cholesteryl-p-toluenesulfonate and tetraethylene glycol, to produce 3-O-(11-hydroxy-3,6,9-trioxaundecyl)cholest-5-ene (tetra-EC) (3). The above steps were carried out with methods reported previously. The coupling of the head group and tetra-EC employed a different method, which had been used by others in the coupling reaction of the same head group and cholesterol, by using silver oxide as the catalyst instead of silver carbonate. Methyl [3-O-(3,6,9-trioxaundecyl) cholest-5-en-3β-yl-2,3,4-tri-O-acetyl-β-D-glucopyranosid]uronate (4) was produced from the coupling reaction with a yield estimated to be ~ 50%, higher than that of the reaction with silver carbonate as the catalyst. The final step was to remove the methyl group and the acetyl protecting groups on the head group by using excess NaOH in a specific solvent system and acidifying with HCl, to obtain crude 3-O-(3,6,9-trioxundecyl) cholest-5-en-3β-yl-β-D-glucopyranosiduronic acid (5). The crude acid product was primarily purified by adjusting the pH of the suspension of the acid in warm ethanol and water and the salt form was obtained. The salt product, (6), was precipitated pure from chloroform solution by addition of mixed ethyl acetate and hexane.

The product (tetra-ECG), which has a negative charge on the head group, was used with other lipids to prepare liposomes. The liposomes, which vary in poly(ethylene glycol) (PEG) chain density and charge location were made for the purpose of mimicking the glycocalyx region in actual biomembranes. Particle electrophoresis was used to measure the mobilities of the liposomes in the solutions with variation of pH (1.8-9.9), ionic strength (0.001M-0.1M) and PEG chain density (0-60% by molar ratio). The classical theory for particle electrophoresis was applied to calculate the mobility and the apparent charge density of the liposomes. The pK_a of tetra-ECG was determined with a plot of the mobility of the tetra-ECG-containing liposome against pH on the surface of the particle. A numerical model, which has been developed as a computational program, was used to interpret the results of electrophoresis as a function of ionic strength, in terms of several parameters which describe the surface properties of the liposomes.

TABLE OF CONTENTS

LIST OF FIGURES

LIST OF TABLES

ABBREVIATIONS

CI	chemical ionization
Chol.	cholesteryl or cholesterol
d	doublet (in NMR results)
DCI	desorption chemical ionization
DPPG	dipalmitoyl phosphatidyl glycerol
egg PC	egg phosphatidylcholine
EI	electron ionization
HPLC	high pressure liquid chromatography
LSIMS	liquid secondary ion mass spectrometry
m	multiple (in NMR results)
NMR	nuclear magnetics resonance
PEG	poly(ethylene glycol)
s	singlet (in NMR results)
tetra-EC	tetraethoxycholesterol
tetra-ECG	sodium [3-O-(3,6,9-trioxaundecyl)cholest-5-en-3β-yl-β-D-glucopyranosid]uronate
tetra-ECPG	Methyl [3-O-(3,6,9-trioxaundecyl)cholest-5-en-3β-yl-2,3,4-tri-O-acetyl-β-D-glucopyranosid]uronate
TLC	thin layer chromatography
tr	triplet (in NMR results)
tri-EC	triethoxycholesterol
qt	quartet (in NMR results)

ACKNOWLEDGEMENTS

I would like to express my special thanks to my supervisor, Don Brooks, for his patience, assistance and encouragement throughout this work. I am especially grateful to Johan Janzen, who has helped me so much during almost all my project. Thanks to everyone in this group for their valuable suggestions and assistance.

Chapter 1

1.0 Objectives

The objectives of this project are:

1) to modify the synthesis of a model lipid which has a cholesteryl base, poly(ethylene glycol) (PEG) chain and glucuronic acid head group;

2) to prepare liposomes, which have different (negative) charge location and different densities of PEG chains, as models of the glycocalyx region in actual biomembranes;

3) to use particle electrophoresis to measure the mobilities of the charged liposomes and apply both the classical theory and a numerical model of liposomes to interpret the results.

1.1 Introduction

Biological membranes are directly involved in many biological processes of living organisms. They are composed primarily of lipids and proteins, with some associated oligosaccharides and small amounts of mono- and divalent ions binding to ionic groups of lipids and proteins, and water. For more than 50 years, biomembranes have been extensively studied in order to understand the relationship between their structure and the function (1, 2). In 1925 Gorter and Grendell (3) first described the structure of a biomembrane as a bilayer lipid matrix. Since then, various models have been proposed to describe membrane organization, resulting in our present understanding of membranes described by the Singer and Nicholson fluid mosaic model (4), which has been proved to be useful for presentation of

the gross organization and structure of lipids and proteins in biomembranes. *Figure* 1.1 is a diagram which is based on the model given by Singer et al. and modified to include a description of carbohydrates on the surface of the membranes (2).

1.1.1 Lipids in Biomembranes

Biological membranes contain an astonishing variety of lipids, both in amount and in kind. Phospholipids are usually found in biological systems, as well as sphingolipids, glycolipids and steroids. Not only do lipids function as a matrix for association of membrane proteins and provide a permeability barrier between the exterior and interior of a cell, they also participate in a variety of specialized biological processes (5).

1.1.2 Chemical Structure of Lipids in Biomembranes

Generally the structure of lipids in biomembranes consists of two parts: a polar or hydrophilic region, and a nonpolar or hydrophobic region. The chemical nature of these two sections can vary substantially. In water the polar regions tend to orient toward the aqueous phase while the nonpolar regions are withdrawn from water. For phospholipids bearing two alkyl chains the lowest free energy is achieved through formation of a two dimensional bilayer which is the basis of biological membranes.

In some cases, models of lipids may be described to have a third part, the spacer region, between the terminal of the hydrophilic head group and the hydrophobic tail in a bilayer or micelle (6). In recent work on the synthesis of artificial lipids, poly(ethylene glycol) (PEG) has been applied as a spacer (7).

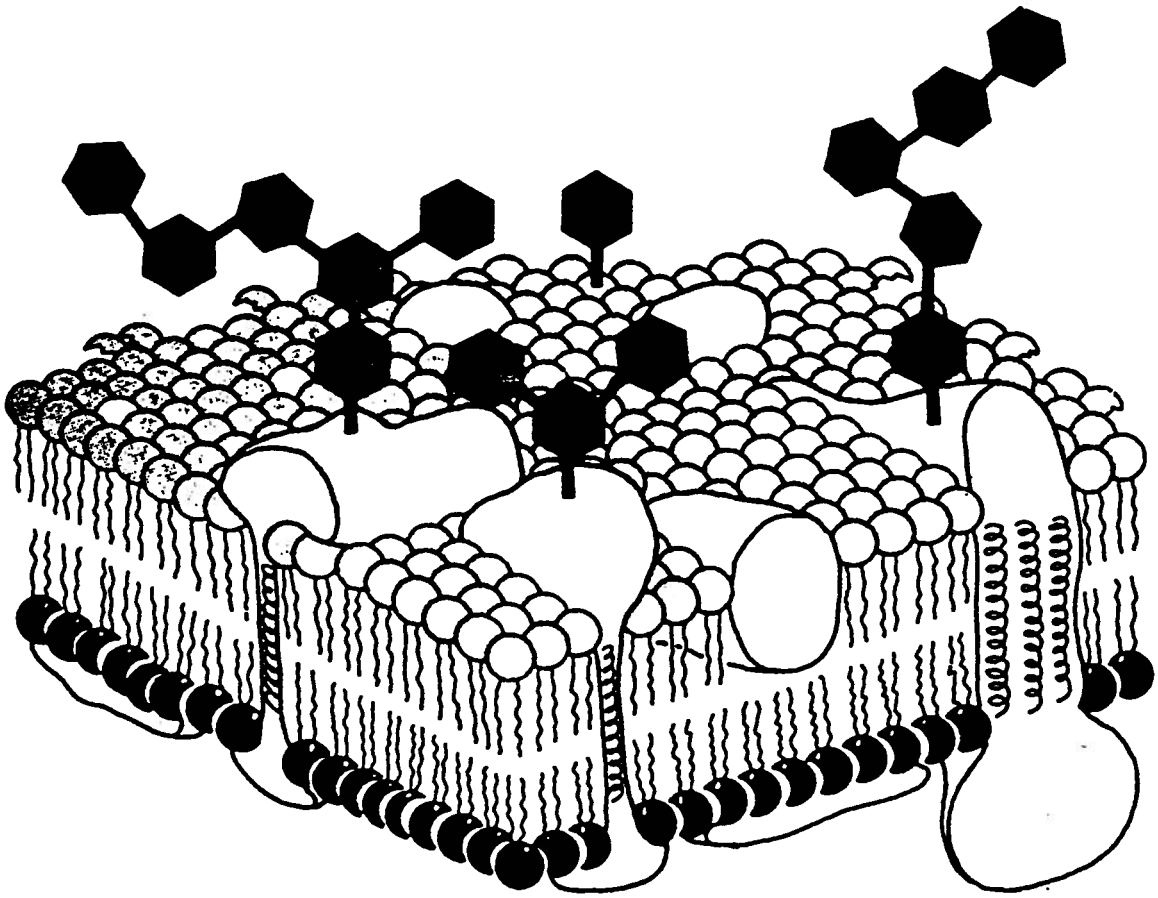

Figure 1.1 A modified fluid mosaic model of biomembrane(2)

It offers a three-dimensional and cross-sectional description of protein, lipid and carbohydrate in the model of a biomembrane. Lipid and protein form a structural bilayer matrix and carbohydrate moieties extend from the surface of membranes into the aqueous solution.

Another characteristics of most lipids is that they have charged head groups, such as phosphate, sulfate, and carboxylate (anionic), as well as ammonium groups (cationic) (8). These provide biomembranes which contain such lipids with net surface charges.

1.1.3 The Model Lipid

Our synthesis of lipids is aimed at making liposomes to mimic biomembrane structures to allow studies of the properties of a model biomembrane surface. The detailed purpose is described in *Chapter* 2.

The model lipid consists of three sections:

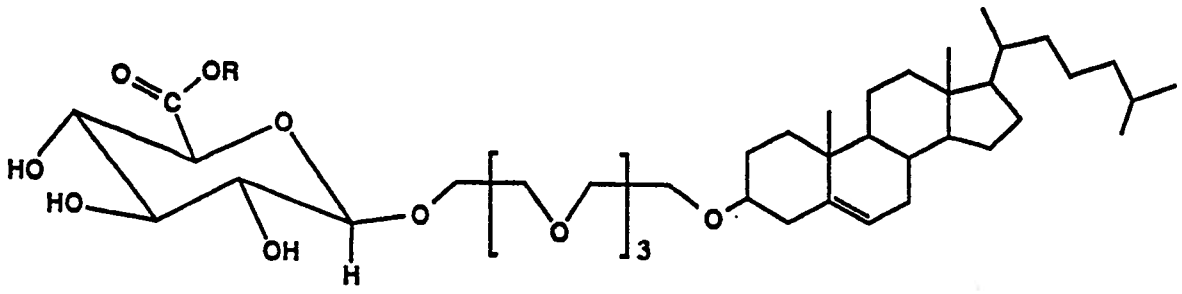

Figure 1.2 The Model Lipid

R = H [3-O-(3,6,9-trioxaundecyl)cholest-5-en-3β-yl-β-D-glucopyranosid]uronic acid

R = Na sodium [3-O-(3,6,9-trioxaundecyl)cholest-5-en-3β-yl-β-D-glucopyranosid]uronate

The cholesteryl group is placed as a hydrophobic anchor in this lipid, because it is present in a wide variety of biological membranes and participates actively in many biological processes (9).

The hydrophilic section is glucuronic acid, which provides the saccharide character. It has been widely observed that carbohydrates on the surfaces of biomembranes are common groups in living organisms. In general they can act as recognition reactants, structural materials and energy stores and are involved in a multitude of interactions with other organisms and biological reagents (10, 11). They are also considered to stabilize the membranes against disruption in some biological systems (12).

The spacer section of the model lipid is PEG, because it is soluble in water and most organic solvents and apparently has a high compatibility with biological systems (13). A compound with four ethylene glycol units was chosen. This particular lipid had been synthesized by Paula J. Sather, a previous student in our laboratory, in 1990 (7). However, she obtained a low yield and was unable to isolate enough product to be used in model membrane studies.

1.2 Methods

The synthesis of the model lipid employed modifications of the procedure described in P.J.Sather's thesis (7). It consisted of three major steps:

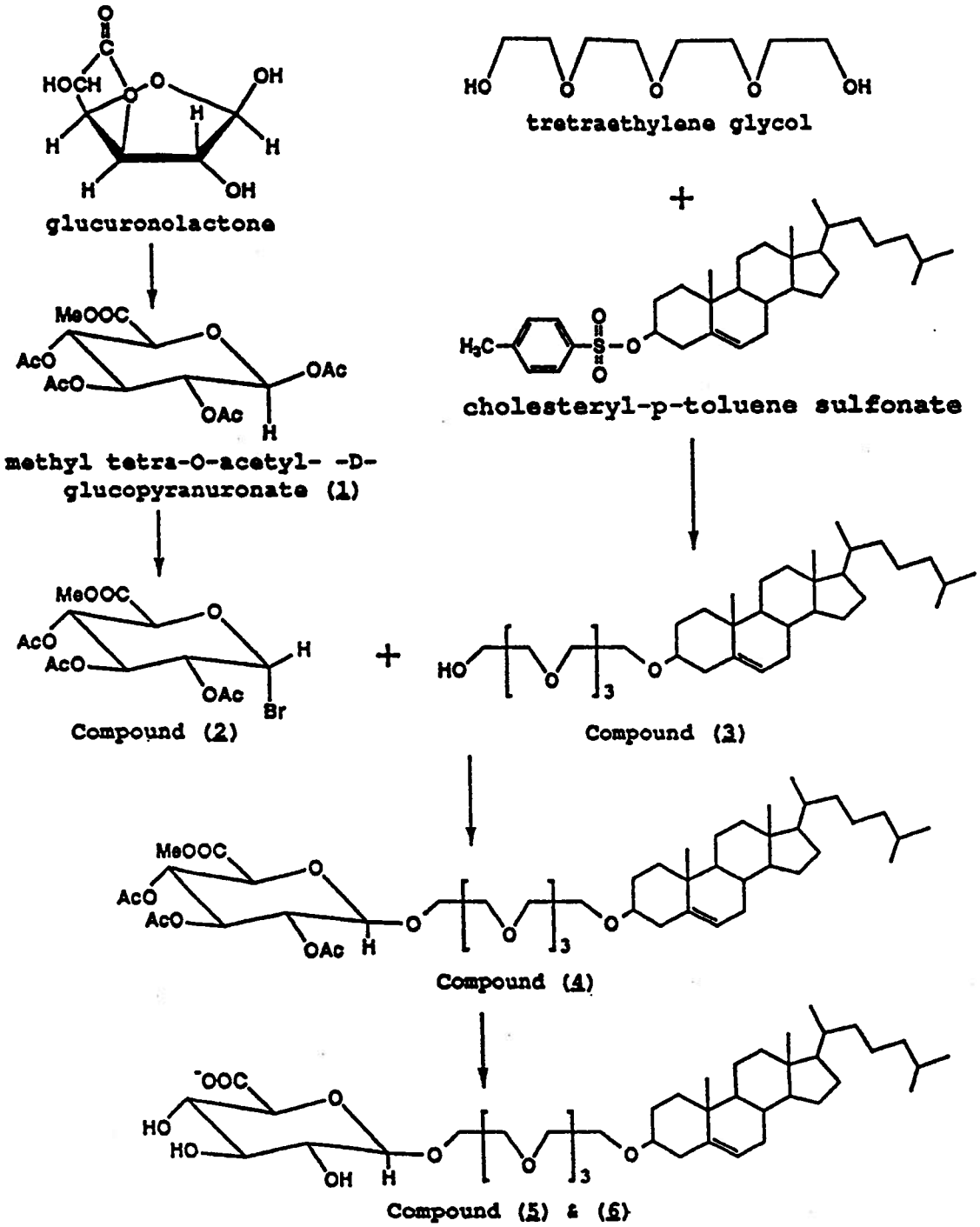

Figure 1.3 Procedure of Lipid Synthesis

The first step is connection of tetra-ethylene glycol to the cholesteryl group by displacing the tosylate from cholesteryl-p-toluene sulfonate. The second step is coupling between compound (3) (tetra-EC) and the protected and brominated glucuronic acid - compound (2), and the final step is removal of the protecting acetyl groups from the glucuronic moiety.

1.2.1 Synthesis of Tetraethoxycholesterol(tetra-EC)

The starting materials, tetraethylene glycol and cholesteryl-p-toluene sulfonate, are commercially available. Cholesteryl-p-toluene sulfonate has very high reactivity with the compounds which contain hydroxyl groups, especially with water. For this reason, the reaction between tetraethylene glycol and cholesteryl-p-toluene sulfonate is carried out under anhydrous conditions and in the absence of oxygen. This method was reported by Brockerhoff and Ramsammy (14). Patel et al. (15) used it to synthesize triethoxycholesterol (tri-EC) and the yield was >90%. Sather (7) applied the same procedures to make a series of oligo-ethoxy-cholesterols and reported the yields given in *Table* 1.1.

From Sather's work, a key to a high coupling yield was to use anhydrous 2,4-dioxane (which had been dried with sodium metal and then distilled prior to the reaction) as the solvent.

Liquid chromatography of mixed organic solvent systems on silica gel columns is the usual way of purification of these compounds. The yield of this procedure was 58.9%.

Table 1.1 Brief Review of Recent Syntheses of PEG-Cholesterol Derivatives

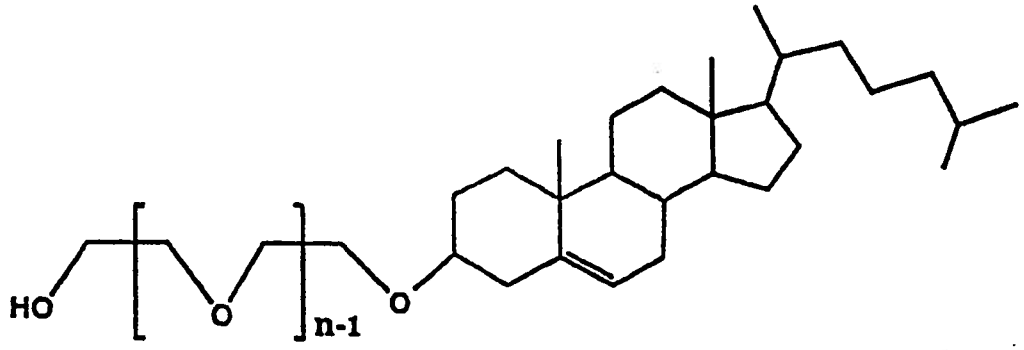

REFERENCE	Ethoxy Unit (n)	Reaction Pathway	Molar Ratio of Reagents: CTS*/PEG	Reaction Time (hr)	Yield (%)
(14)	3	*a*	--	--	--
(15)	3	*b*	1 / 25.3	2	92
(16)	1	*b*	1 / 25-30	2-4	81
	3	*b*	1 / 25-30	2-4	92
(20)	3	*b*	--	2-3	--
(13)	3	*b*	1 / 25.4	24	~100
	4	*b*	1 / 4.5	24	56.5
	6	*b*	1 / 5	60	26
(18)	3	*b*	--	--	--

a reported by Fong et al in *Lipids*, Vol.12, 10, 857-62(1977)

b excess PEG and cholesteryl-*p*-toluenesulfonate were stirred in reflux of dioxane(dried by reflux with Na) for several hours under N_2 [Patel et al, 1984, Ref. (15)]

* CTS: cholesteryl-p-toluene sulfonate

1.2.2 Synthesis of Protected and Brominated Glucuronate (2)

Two steps are taken to obtain the compound (2) (*See Figure* 1.3). They were reported initially by Bollenback et al. (17) in 1955 and utilized widely since then as the traditional method to make this compound (7).

The first step includes esterification of glucuronolactone (to produce methyl glucuronate) and acetylation of the four hydroxyl groups with acetic anhydride. The solvents are anhydrous methanol and pyridine, the latter acting as a catalyst of acetylation. In this part, the crude product is obtained by crystallization at ~ 4°C from the solution of the reaction mixture and the pure crystals are obtained by recrystallization in absolute ethanol. Sometimes the color of the reaction mixture is so dark that the solution of crude product needs to be decolorized by carbon (reflux under reduced pressure) to remove the colored impurities before recrystallization.

Compound (1) has two anomers: α and β(*See Figure* 1.4). The product has been reported to be the β anomer based on the NMR evidence (7). In our work the yield was 33.5%.

α type β type

Figure 1.4 Two Anomers of Compound (1)

The second step of the synthesis of compound (2) is bromination at the anomeric carbon of compound(1). Hydrobromic acid in glacial acetic acid (30% by weight) reacts with the acetyl group, eliminating one molecule of AcOH and forming the C-Br bond. The crude product is crystallized with absolute ethanol.

The product was α anomer of compound (2) (because of the anomeric effect of the suger ring) and the yield was 85% in Bollenback et al.'s work and 73% in our synthesis. The ^{1}H NMR spectrum of the product in *Figure* 1.5 indicates, from the coupling constant between the protons connected directly to the sugar ring, that the bromine is axial in product (18) - that is the α anomer of compound (2). (*See* Appendix II)

The procedure of bromination had also been used by Sather (7) with very satisfactory results. An important point is that the brominated compound (2) should be used in the next coupling reaction as soon as possible because the Br is sensitive to both oxygen and water, especially in light and heat, which might produce the impurities that could complicate subsequent reactions.

1.2.3 Coupling Reaction

Typically, catalysts are used in the coupling reaction between the brominated sugar and tetra-EC to activate the bromine first; then the sugar is attacked by the hydroxyl group on tetra-EC to form the ether linkage. Koenig Knorr's method was the first one dealing with this type of coupling, with silver carbonate as the catalyst (*See Figure* 1.5). Again, Sather followed this method in her work, but the yields reported were very low, around 30% or less, after purification by column chromatography (7).

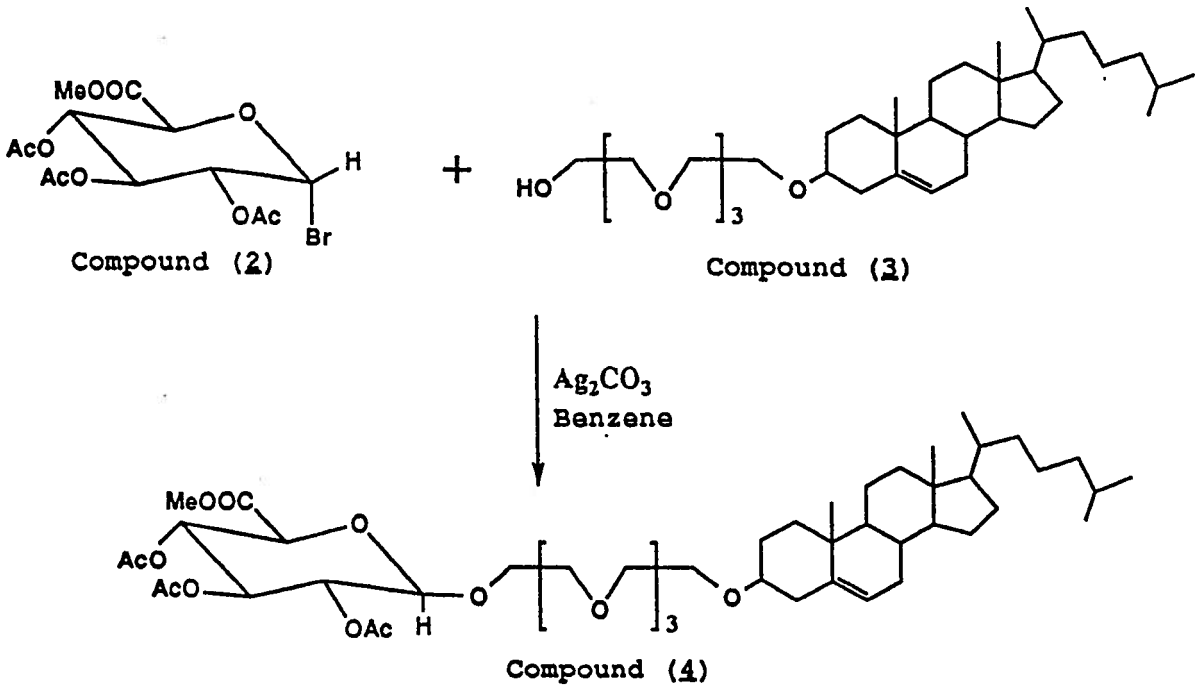

Figure 1.5 Koenig-Knorr Coupling Reaction

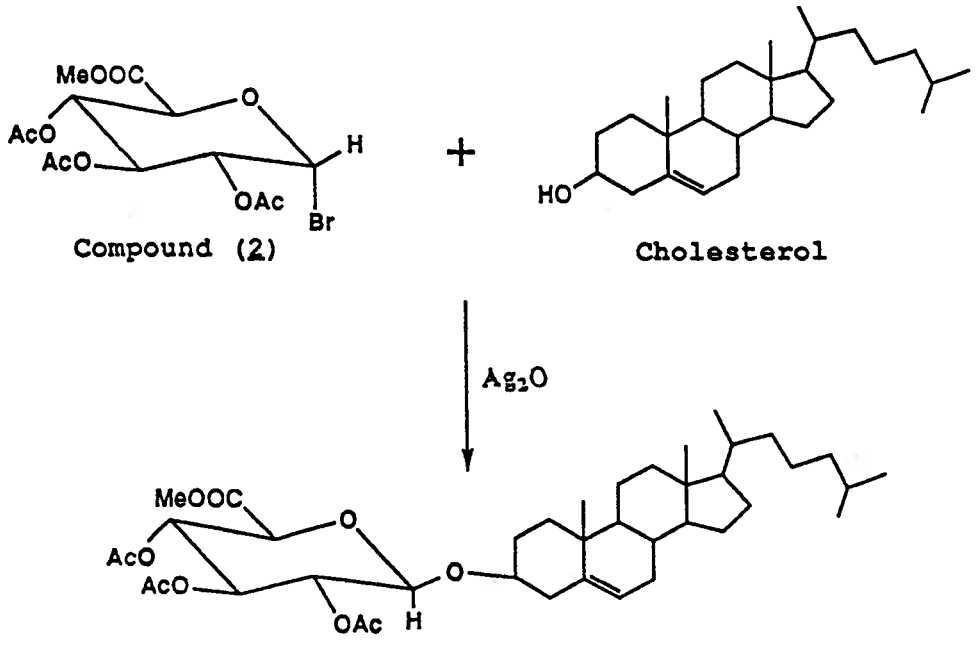

Figure 1.6 Scheme of Schneider et al.'s Coupling Reaction (20)

This method was considered and tried in our project. The coupled product did form, but the yields varied from a few percent to less than 30%, similar to Sather's results. Even though silver carbonate was freshly made and dried in the dark (which did affect its catalytic efficiency), there was no significant improvement in the yield.

A mixed catalytic system of mercury bromide and mercury oxide, based on Goodrich et al.'s work (19), was tried in our system, but the results were also not satisfactory.

Another approach was an older method reported in 1969 by Schneider and Bhacca (20), which had been used in Goodrich et al.'s previous work (21) (*See Figure* 1.6). In this method, silver oxide (freshly made) had been used instead of silver carbonate. The reaction was between exactly the same sugar used in our system, and simple cholesterol. The yield reported by Schneider et al. was very high (and so was the yield of their deprotection reactions).

This method was applied in our system and brought the yield of coupling reaction of the sugar and tetra-EC up to ~50%. (The yield was estimated from ^{1}H-NMR spectra of several samples of impure products, because of the difficulty of purification).

The crude product was a syrup which was easily dissolved in an organic solvent. Silica gel provided an appropriate stationary phase to separate the compounds in liquid chromatography. (Aluminum oxide column was tried and proved inadequate) The problem in the purification is that both tetra-EC and the product (3), tetra-ECPG, have very strong affinity for silica gel. Even though they can be separated very well on TLC silica plates in small scale, with the mixed solvent system of ethyl acetate, chloroform and hexane, the separation on a column was quite different because the product, tetra-ECPG, always came off contaminated with a small

amount of tetra-EC (as detected by TLC). Controlling the amount and manner of loading material did not improve the separation. The pure product had to be collected from only a few of fractions in each run of chromatography, since most of the fractions remained as mixtures of the product and tetra-EC (by TLC results). The practical reaction yield, >50%, was estimated roughly from the sum of the pure product and the product which remained in the mixture with tetra-EC. For determination of the molar ratio of tetra-ECPG and tetra-EC in the mixtures, the method is described in Appendix II. TLC analysis of the mixtures indicated that most of the components were those two compounds.

The yield from the purification was so low that several chromatography runs had to be made, starting from a few grams of the crude product, to provide sufficient material for the next step.

1.2.4 Deprotection

In organic syntheses, it is an old problem to make specific functionalized compounds by retaining some of the functional groups while changing others in reactions. Many reagents have been applied in protection, deprotection or catalysis for both of these two reactions under different circumstances.

In our project, deacetylation and deesterification were required. The latter is easy to be approached by hydrolysis (13, 19, 20). However, the deacetylation step took much more effort. Although there have been many methods of deacetylation used, with sodium methoxide in methanol as the most commonly used reagent system (22), most of them were applied only for small molecule systems.

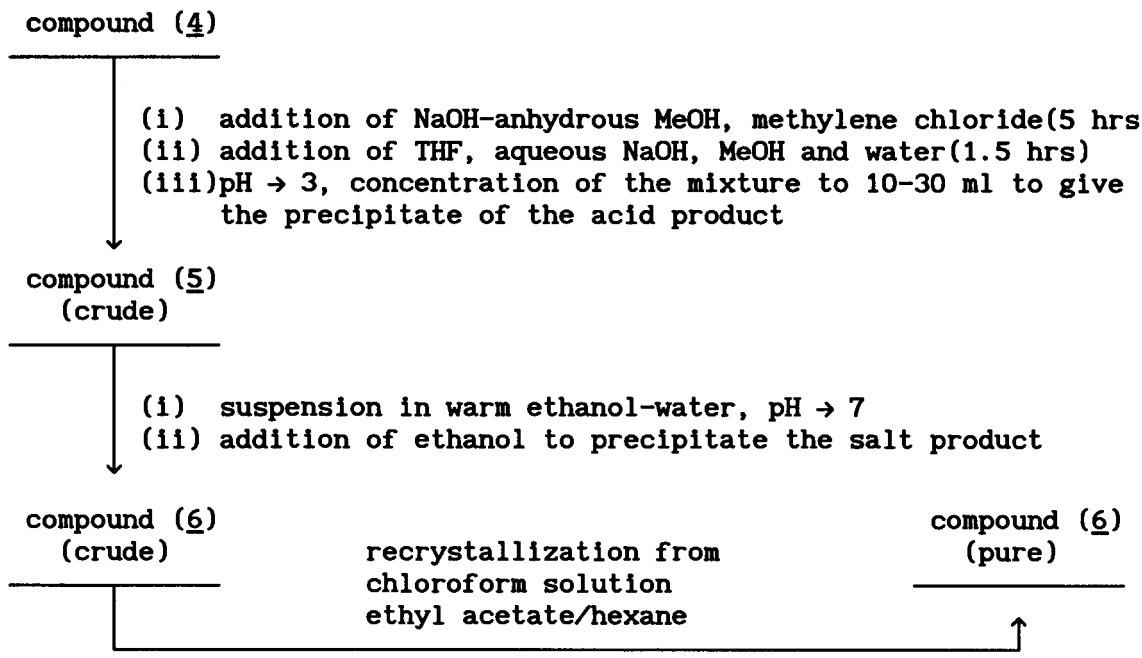

Figure 1.7 A diagrammatic description of the procedure of the deprotection of the compound(4)(tetra-ECPG)

A procedure, which had been reported by Schneider et al. (20) and used in Sather's deacetylation step (7), was first applied in deacetylation of compound (4). It is a complex system of NaOH in anhydrous methanol (sodium methoxide), methylene chloride, THF and then aqueous NaOH solution. The procedure is described in *Figure* 1.7. Following adjustment of the pH to 3, the crude acid product is separated from the mixture by centrifugation. The primary purification is transformation of the crude acid (5) to the salt (6) by adjusting pH to 7 in aqueous ethanol. This step removes the impurities which are not soluble in water and ethanol.

The procedures, including the quantities of reagents given, were exactly followed, but the reactions did not go to completion (*See the TLC results in Figure* 1.8). A series of other compounds appeared, making purification very difficult and greatly lowering the deprotection yield. Longer reaction times produced no improvement in the results. It seems that some uncompletely deprotected compounds form producing poor yields. These compounds were identified because the amounts were very small.

After several failures, the sodium hydroxide concentration in the first part of the reaction was increased. The yield of crude material was improved. After the primary purification, further purification again became a significant problem because of the polyhydroxylated nature of the compounds (5) and (6). (*See Section* 1.3 TLC results).

TLC showed that the deprotected product interacted strongly with silica gel for both acidic and salt forms. In the usual (not highly polar) solvent systems, the product (acid or salt) almost always remained at the origin of the plate. The product dot moved from the origin when a polar solvent, e.g., methanol, was added, but the solubilities of the products were limited in methanol. Hence, chromatography on a silica gel column was not considered for the purification.

Instead, recrystallization of the salt product, compound (6), from chloroform (which is the best solvent for the products) was attempted, with solvents which were expected to lower the solubility of the product and crystallize them from solution. A precipitate, which was the pure product, resulted upon addition of a mixed solvent of ethyl acetate and hexane. TLC gave an indication of its purity. The integration information from proton NMR and LSIMS results in different matrices were also useful.

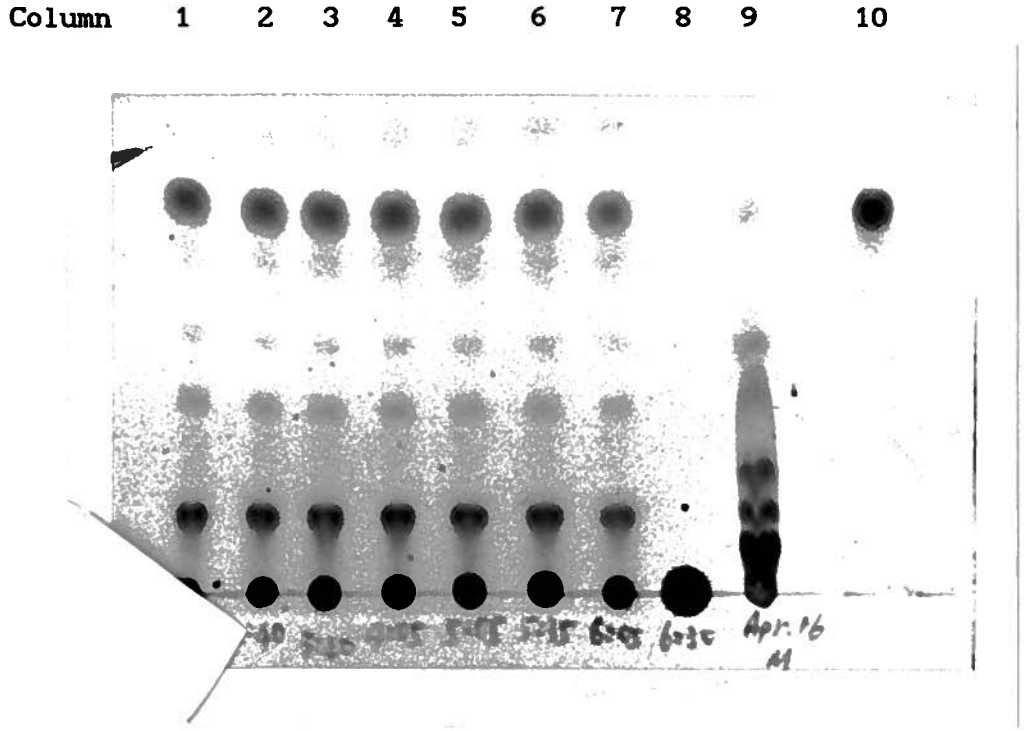

Figure 1.8 TLC Results for the Compounds in the Deprotection Step (solvent system: ethyl acetate/chloroform/hexane 3:3:1)

Columns 1 ~ 7 are the results of TLC monitoring of the first 5-hour reaction (*See Figure* 1.7), with sampling times indicated below. Column 8 is the result for the sample taken from the reaction system after addition of aqueous NaOH solution. Column 9 is for the mixture extracted from the finished reaction solution with chloroform, in which there are a series of compounds. Column 10 is the reference of the compound before deprotection.

The yield from this procedure was 32.6%, but not all of the product was recovered. A portion of the product remained in solution with the impurities.

The practical yield of the reaction was not estimated, therefore, because it was difficult to determine the type and concentration of the impurities. The NMR analysis of pure deprotected product (6) is in Appendix II. The product (6), called tetra-ECG, was used to prepare liposome in the next part of this project.

1.3 Experimental

General Details

Proton NMR spectra were recorded on Bruker WH-400 MHz and Bruker AC-200E (200 MHz) spectrometers in $CDCl_3$ or CD_3OD as the solvent. Mass spectra were recorded on a Kratos MS-40 (EI), a Delsi Nermag R10-10 C Mass Spectrometer (CI & DCI) with ammonia reagent grade gas and a Kratos Concept II HQ Mass Spectrometer(LSIMS) with matrices of glycerol and thioglycerol.

Solvents and reagents were used as purchased with the exception of those listed below:

Chloroform (solvent for making tetra-EC), benzene, pyridine, dichloromethane and tetrahydrofuran (THF) were distilled prior to use. Dioxane was distilled from a reflux with sodium for 1 hour prior to use. Methanol was distilled from a reflux with magnesium and iodine for 0.5 hours, stored over 4Å molecular sieves, and distilled again from calcium hydride or sodium hydride, prior to use. Cholesteryl-p-toluene sulfonate, tetra-ethylene glycol, and glucuronolactone were dried under vacuum. Ag_2O

was made from hot NaOH and $AgNO_3$ solution in the dark and dried prior to use. Ag_2CO_3 was made from $AgNO_3$ and Na_2CO_3 solutions in the dark.

SYNTHESES

Preparation of Methyl (1,2,3,4-tetra-O-acetyl-β-D-glucopyran)uronate (1)

This reaction was based on the procedure described by Bollenback et al. (17), and also by Sather (7). The reagents and amounts were:

Glucuronolactone	10 g, 56.78 mmol
Sodium hydroxide	0.08 g(in MeOH)
Anhydrous methanol	75 ml
Acetic anhydride	60 ml
Pyridine	25 ml in 5 ml acetic anhydride

The product was decolorized with carbon if necessary and recrystallized from absolute ethanol. The yield was 7.15 g, 19.00 mmol.

^1H NMR (400 MHz) $CDCl_3$ 2.03(2s,9H), 2.11(s,3H), 3.73(s,3H), 4.16(d,1H), 5.12(tr,1H), 5.26(m,2H), 5.76(d,1H)

Mass Spectrum DCI: m/e 394$(M+NH_4)^+$, m/e 317$(M-59)^+$, m/e 257$(317-59-H)^+$ m/e 228$(257-O-CH)^+$, m/e 114$(317-3x59-2CH)^+$ or $(257-O-CH)^{++}$

Preparation of Methyl (2,3,4-tri-O-acetyl-α-D-glucopyranosyl bromide) uronate (2)

This reaction procedure was also from Bollenback et al. (17). The reagents and amounts were:

Compound (1)	1.8114 g, 4.813 mmol
Hydrobromic acid (30% in acetic acid)	7.2 ml(in 3.6ml)
Chloroform	30 ml
Sodium bicarbonate (saturated)	30 ml

After reaction and removal of acetic acid, the crude product dissolved in chloroform was washed with $NaHCO_3$ saturated solution and then water to remove the residual acid. The product was recrystallized from 100% ethanol. The yield was 1.389 g, 3.497 mmol.

^1H NMR (400 MHz) $CDCl_3$ 2.04(2s,6H), 2.09(s,3H), 3.75(s,3H), 4.57 (d,1H), 4.84(qt,1H), 5.22(tr,1H), 5.59(tr,1H), 6.62(d,1H)

Preparation of 3-O-(11-hydroxy-3,6,9-trioxaundecyl)cholest-5-ene (3)

Tetraethylene glycol (11.0162 g, 56.7 mmol), cholesteryl-p-toluene sulfonate (0.9928 g, 1.836 mmol) and dioxane (20 ml) were added to a 50 ml round bottom flask. A condenser was added and the mixture was stirred at reflux under a nitrogen atmosphere for 6 hours (after 3 hours the reaction was finished according to the results of TLC). The dioxane was removed by rotary evaporation and the residue was dissolved in 30 ml water and extracted with diethyl ether (5 x 80 ml) in a 250 ml separatory funnel. The organic extracts were combined, washed with 10% Na_2CO_3solution (1 x 40 ml), and then water (5 x 60 ml). The organic phase was dried over anhydrous sodium sulfate, filtered and the filtrate was evaporated under reduced pressure. The residue was loaded onto a silica gel column (20 g), packed with 1:1 (volume ratio) ethyl acetate/chloroform. The column was eluted with the same solvent system and the product was collected in 1 ml fractions (each fraction was analyzed by TLC). The fractions containing product were combined and evaporated under reduced pressure to give 0.609 g, 1.082 mmol of product.

TLC R_f= 0.24 , silica 60, ethyl acetate/chloroform 1:1(by volume ratio)

^{1}H NMR $CDCl_3$ (400 MHz) 0.64(s,3H), 0.84(qt,6H), 0.88(d,3H), 0.97(s,3H), 0.98~2.40 (m, ~29H), 3.16(m,1H), 3.60~3.75(m, ~16H), 5.32(d,1H)

Mass Spectrum EI m/e 560$(M-2)^+$, m/e 368$(M-194)^+$, m/e 353$(368-CH_3)^+$, m/e 255$(368-113_{\text{side chain}})^+$, m/e 247$(368-C_9H_{13})^+$, m/e 195$(M-368+H)^+$

DCI(NH_3) m/e 581 & 580$(M+NH_3)^+$, m/e 563$(M)^+$, m/e 369$(M-193)^+$, m/e 353$(369-CH_3-1)^+$, m/e 195$(M-368+H)^+$

Preparation of Methyl [3-O-(3,6,9-trioxaundecyl)cholest-5-en-3β-yl-
-2,3,4-tri-O-acetyl-β-D-glucopyranosid]uronate (4)

Compound (3) (0.4642 g, 0.8247 mmol), (2) (1.2415 g, 3.126 mmol), freshly made silver oxide (0.3919 g, 1.691 mmol) and benzene (10 ml), were stirred together at room temperature in a 25 ml round bottom flask in the dark. After 24 hours, adding a few grams of Celite, the mixture was filtered and the filtrate evaporated under reduced pressure to remove solvent. The residue was separated on a silica gel column (100 g) packed with ethyl acetate/chloroform/hexane 3:1:2 (by volume ratio). The column was eluted with the same solvent system, and 1 ml fractions were collected and monitored by TLC. The crude product, which by TLC contained mostly unreacted (3) and the product (4), was 0.6523 g. From ^{1}H NMR, the molar ratio of (3) and (4) was calculated to be 1.15-1.4. The practical yield of the product (4) was 0.397-0.433 mmol, 0.349-0.381 g.

The crude product was purified with about 10 runs of the same chromatography as above, and the pure product was obtained.

^{1}H NMR $CDCl_3$ (200 MHz) 0.65(s, 3H), 0.83(d, 3H), 0.85(d, 3H), 0.89(d, 3H), 0.98(s, 3H), 1.0~2.4(~29H), 1.98,2.00 & 2.02(3s, 9H), 3.62(~16H), 3.74(s, 3H), 4.03(d, 1H), 4.65(d, 1H), 4.99(tr, 1H), 5.22(2tr, 2H), 5.32(d, 1H)

TLC (pure product) R_f = 0.45, silica 60,

ethyl acetate/chloroform/hexane 3:1:2 (by volume ratio)

Mass Spectrum (pure product) DCI (NH_3)

m/e 929$(M+2NH_3+NH_4)^+$, m/e 913$(M+NH_3+NH_4)^+$, m/e 897$(M+NH_4)^+$, m/e 877$(M-1)^+$, m/e 837$(M-CH_2CO+1)^+$, m/e 528$(M+NH_4-368)^+$, m/e 396$(528-3C_2H_4O)^+$, m/e 368(Chol.-16)$^+$, m/e 352$(396-C_2H_4O)^+$, m/e 336$(352-O)^+$, m/e 334$(352-NH_4)^+$, m/e 317$(334-O-1)^+$, m/e 308$(352-CH_3CO-1)^+$, m/e 292$(308-O)^+$, m/e 276$(292-2O)^+$, m/e 257$(276-NH_4-1)^+$, m/e 234$(276-CH_3CO+1)^+$, m/e 218$(234-O)^+$, m/e 216$(234-NH_4)^+$

Preparations of [3-O-(3,6,9-trioxaundecyl)cholest-5-en-3β-yl-β-D-glucopyranosid]uronic acid (5) and Sodium [3-O-(3,6,9-trioxaundecyl)cholest-5-en-3β-yl-β-D-glucopyranosid]uronate (6)

(4) (0.460 g, 0.524 mmol) was dissolved in anhydrous ether (6 ml) and dichloromethane (6 ml). 0.5 N sodium hydroxide in anhydrous methanol (0.48 ml, 0.24mmol) was added and the reaction was carried out at room temperature, monitored by TLC. After 4 hours, it was found by TLC with solvent system of ethyl acetate/chloroform/hexane 3:1:2 that a series of compounds formed . 0.7ml sodium hydroxide-methanol (0.66 N, 0.462mmol) was added. After 1 hour further, TLC showed only one product. THF(40 ml) was added with initiation of stirring, followed by addition of aqueous 1 M sodium hydroxide (12 ml, 12mmol) in one portion and methanol (35 ml).

Finally water (75 ml) was added slowly. Stirring was continued for another 1.5 hours at room temperature. The pH of the solution was adjusted to 3 with the addition of 10% HCl. The solution was concentrated with difficulty by rotary evaporation under reduced pressure to about 10-30 ml. The precipitate was centrifuged and the supernatant was concentrated again to provide more material. The precipitate, the crude acid (5), was suspended in warm aqueous ethanol and sufficient aqueous sodium hydroxide was added to adjust the pH to around 7 at which point all the acid had dissolved. Ethanol was added and the salt precipitate formed and separated with centrifuging. The yield of crude salt (6) was 295.9 mg. The crude product (6) was dissolved in chloroform and then precipitated by ethyl acetate and hexane (3:1, volume ratio). The precipitate was proven by TLC, proton NMR and LSIMS to be pure product (6), 130 mg, 0.171 mmol.

TLC R_f[Salt, (6)] = 0 for:
ethyl acetate/chloroform/hexane 3:1:2, chloroform/ethyl acetate 3:1,
ethyl acetate/chloroform/benzene 10:10:3, chloroform,
ethyl acetate/$CHCl_3$/ethanol 2:2:1,
R_f[Salt, (6)] = 0.56 for methanol, 0.55 for ethanol,
0.17~0.6 for chloroform/methanol 7:1,
0.57~0.86 for chloroform/methanol 1:1,
0.39~0.48 for ethyl acetate/methanol 6:1;
R_f[Acid, (5)] = 0 for chloroform/methanol 7:1,
0.07 for ethyl acetate/methanol 6:1

^1H NMR $CDCl_3$ 0.65-2.40(cholesteryl section, ~46H by integration), 3.0-4.8(broad, ~24H), 5.34(d, 1H)

LSIMS (low resolution) matrix: thioglycerol

m/e 761(M+1)$^+$, m/e 693(761- COONa)$^+$, m/e 585(M-176$_{\text{sugar part}}$+2C)$^+$, m/e 475(chol.+$CH_2CH_2OCH_2CH_2O$+2H)$^+$, m/e 443(chol.+$CH_2CH_2OCH_2$)$^+$, m/e 413(chol.+CH_2CH_2)$^+$, m/e 369(chol.-16)$^+$

LSIMS (high resolution) matrix: thioglycerol

Mass range: 761-761 No. peaks: 1 Base Int.: 168501

Mass: 761.48241 Carbon 41 Hydrogen 70 Oxygen 11 Sodium 1

(The theoretical formula for the product is $C_{41}H_{69}O_{11}Na$)

1.4 Discussion

In this part of the work, compounds (4), (5) and (6) were produced. *Table* 1.2 is the list of all the products synthesized. However, there are some problems which remained unsolved. The first problem was purification of these types of lipids. Problems occurred in almost all the procedures, from synthesis of tetra-EC through production of the deprotected lipid.

Since the purifications of some of the products are on a hundred-milligram scale, HPLC seems appropriate but optimizing the solvent systems will be very important for improvement of the purification.

Better methods of purification on a milligram scale need to be developed for the deprotected product, tetra-ECG, and an effort should be made to increase the yield of the reaction. Although it has been improved in this work, several methods suggested themselves, based on more recent publications:

(i) OH-resin as a reagent for deacetylation (22).

In this reference, IRA-400(OH) resin was applied in sugar and nucleoside systems to remove acetyl groups with yields of 70% up to 91%.

(ii) Enzymes (23).

It was reported that seven enzymes could catalyze the partial deacetylation of sucrose derivatives in phosphate buffer or phosphate buffer-organic co-solvent with variable yields.

Basically, these two methods were again effective for small molecules and the conditions of the reactions were selected only for the particular circumstances in their syntheses. However, these could be good starting points to improve the deprotection of tetra-ECPG.

Table 1.2 Yield of Products
(*See Figure* 1.3, the procedure of the synthesis)

Product	Catalyst/Solvent	Purification	Yield(%)
(1)	pyridine/$(AcO)_2O$	crystallization (from reaction solution)	33.5
(2)	--/acetic acid	recrystallization (from 100% EtOH)	72.7
(3) tetra-EC	dioxane, N_2	chromatography (ethyl acetate/ chloroform 1:1, silica gel)	58.9
(4) tetra-ECPG	Ag_2O/benzene	chromatography (ethyl acetate/chloroform /hexane 3:1:2, silica gel)	48.1-52.5*
(6) tetra-ECG	--/methanol(etc.)	precipitation (from chloroform solution by ethyl acetate/hexane)	32.6**

* the yield was estimated from ^1H NMR results
** the yield was for the pure product obtained in the experiment

Chapter 2

2.1 Introduction

Liposomes are artificial lipid vesicles which are composed of one or more bilayers and have an aqueous interior or interlameller phase (*See Figure* 2.1). They can be classified into small unilamellar vesicles (SUV), large unilamellar vesicles (LUV) and multilamellar vesicles (MV) by their size and the number of concentric bilayers present (24).

Liposomes are structurally similar to biomembranes and have been utilized as models for studying many aspects of biological membrane properties, e.g., membrane lipid chemistry, lipid-protein interactions, transport phenomena and ligand binding to membranes. They also have been developed as an approach to controlled drug-delivery systems (25).

The liposomes in this work were made from the model lipid synthesized in *Chapter* 1, tetra-ECG, which has a cholesteryl base, a PEG spacer and an acidic monosaccharide head group. While cholesterol does not form bilayers spontaneously, addition of PEG chains allows these molecules to form bilayers and liposomes (15). The liposomes not only have a bilayer matrix of cholesterol derivatives, but also have carbohydrates as well as PEG chains linked on the surface. They therefore can be employed as a model to mimic the behavior of actual membranes using pure molecules with well defined properties. The liposomes are then examined by a technique which is thought to be sensitive to the properties of the head group region, particle electrophoresis. The result is interpreted in terms of a theory for the electrophoretic mobility which contains parameters incorporating the chain concentration, thickness and charge location within the surface region (26).

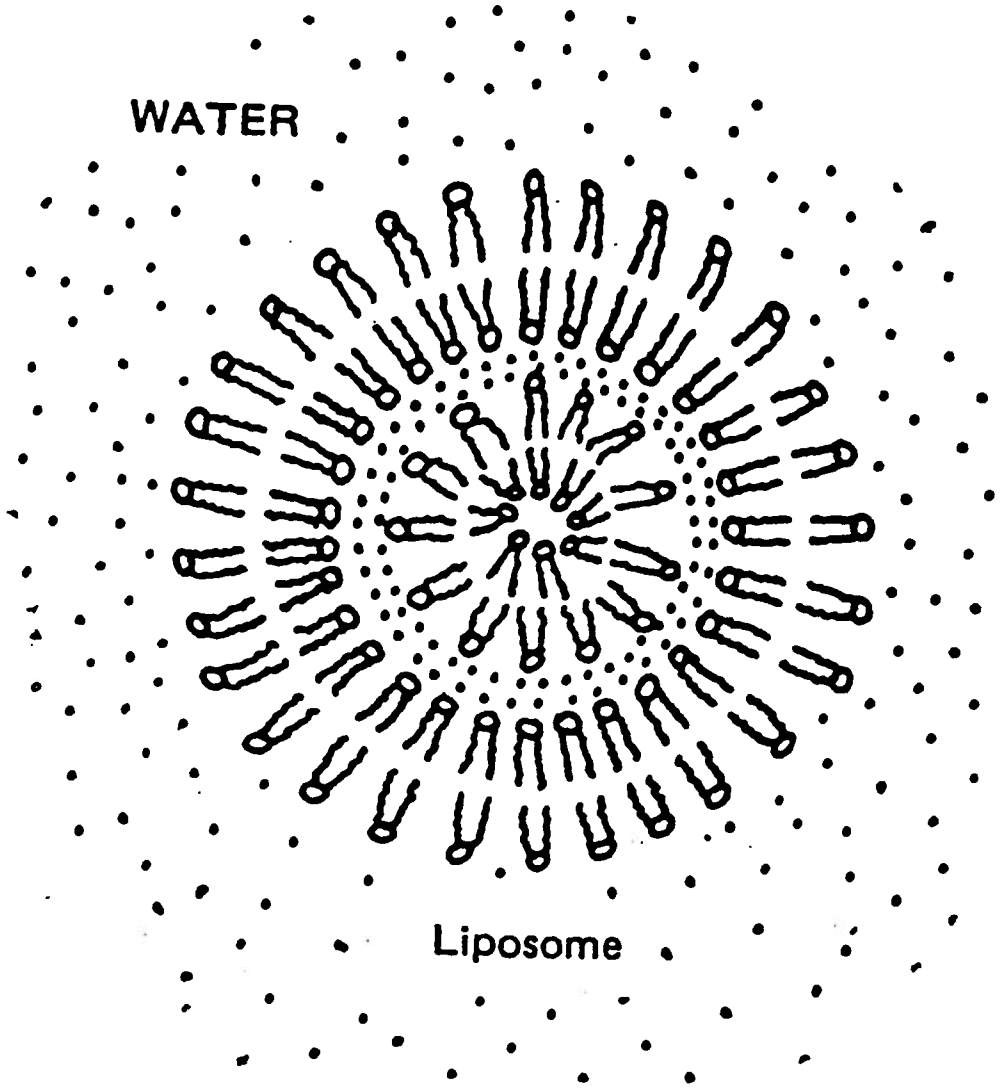

Figure 2.1 Liposome structure (24)

Using the method of particle electrophoresis, the electrophoretic mobility of charged particles in an electric field can be measured. The mobility, which is the particle velocity per unit electric field strength, is related to the physico-chemical properties of the particle surface by the theory described below. Since biological surfaces are normally negatively charged, particle electrophoresis has been used in research on many biological organisms and mammalian cells, especially red blood cells (27). There has been a lot of work which focused on the relationship between the surface properties and behavior of single red cells, using particle electrophoresis. Usually the mobilities are interpreted using theories which apply to smooth charged surfaces. Cell membranes, however, contain many glycolipids and glycoproteins whose head groups extend into solution some distance and carry charged residues which are distributed throughout the depth of the head group region, or glycocalyx. Hence, it is not appropriate to interpret the electrophoretic mobilities of cells with theories which assume smooth charged surfaces.

In this project, particle electrophoresis was applied to liposomes of known compositions with head groups whose properties modeled those found on biological cells. A theory expressly designed for surfaces bearing such structures was used to interpret the results.

2.2 Theories of Particle Electrophoresis

2.2.1 The Theory for Charged Particles with A Smooth Surface

The classical theory for dealing with the behaviour of smooth charged particles, assumed to be locally flat, in electrophoresis is as follows:

An electrical double layer forms near the surface of charged particles because the counterions in solution are attracted to the surface. (*See Figure* 2.2) The electrostatic potential at the surface of charged particles, $\Psi(o)$, is related to the surface charge density, σ, by (29):

$$\Psi(0) = \left(\frac{2kT}{e}\right) \sinh^{-1}\left\{\frac{\sigma}{c_i^{1/2}} \left(\frac{500\pi}{\varepsilon kT}\right)^{1/2}\right\} \qquad [1]$$

which reduces to (27):

$$\Psi(0) = \frac{4\pi\sigma}{\kappa\varepsilon}, \quad \text{if } \frac{ZF\Psi(0)}{RT} \ll 1 \qquad [2]$$

where σ surface charge density(esu/cm^2)

κ Debye-Hückel parameter:

$$\kappa = \left[\frac{8\pi N_{av}\, e^2\, I}{10^3 \varepsilon kT}\right]^{1/2} (cm^{-1}),$$

κ^{-1} is called the electric double layer thickness(cm)

ε dielectric constant of water (78.5)

k Boltzmann's constant (1.3805×10^{-16} erg/$^\circ$K)

N_{av} Avogadro's number (6.025×10^{23})

T temperature ($^\circ$K) (298°K in our experiments)

e electron charge(4.8×10^{-10}esu)

I ionic strength $I = \frac{1}{2} \sum_{ions} C_i Z_i^2$ (M)

C_i molar concentration of i-th ionic species

Z_i valence of i-th ionic species

F Faraday constant $F = N_{av}\, e$

The electrostatic potential decays with distance from the surface of particles; if $\frac{ZF\Psi(0)}{RT} \ll 1$, $\Psi(0)$ is given by (27):

$$\Psi(x) = \Psi(0)\, e^{-\kappa x} \qquad [3]$$

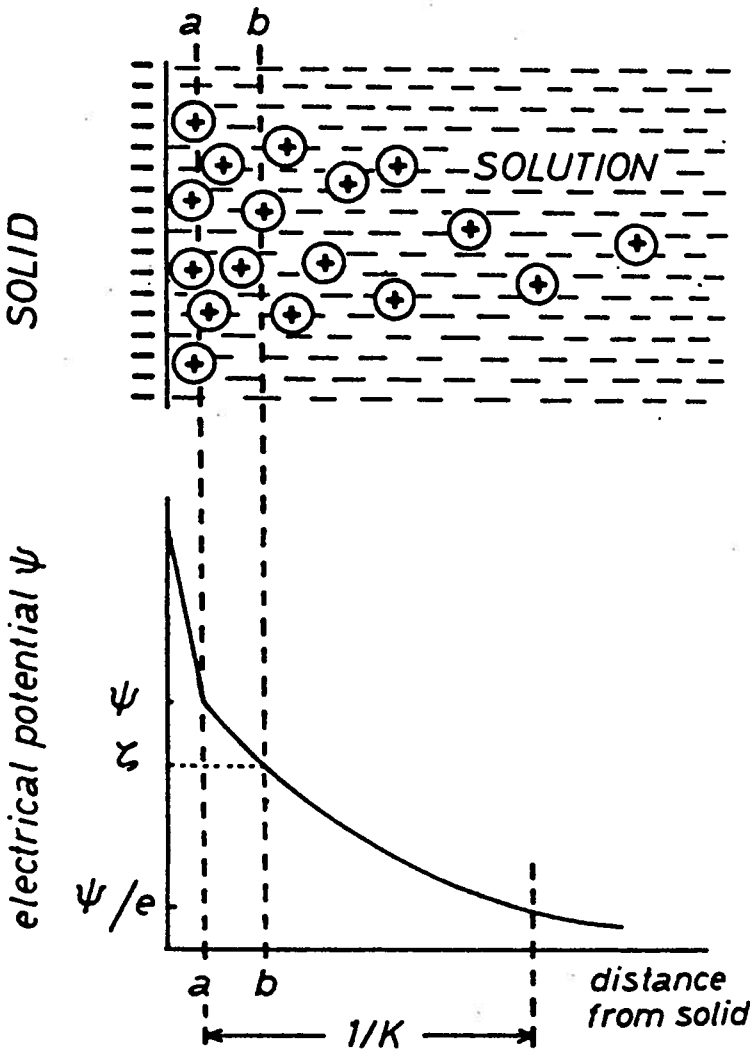

Figure 2.2 Concepts of Electric Double Layer and Electrokinetic Potentail(ζ)

The electric potential, Ψ, decays with the distance. a--the Stern layer of "fixed" charges; b--shearing boundary of the solution when solid moves; $1/\kappa$--electric double layer; ζ--electrokinetic potential or zeta potntial (28)

The motion of the charged particle is determined by the direct electrical force, the fluid drag (from the viscosity of the solution) and the electroosmotic retardation (due to motion of the electric double layer in the electric field in the direction opposite to velocity of the particles). The famous Helmholtz-Smoluchowski formula describes this behaviour, for the case in which the radius of curvature of the particle surface is large compared with $1/\kappa$, the electric double layer thickness:

$$U = \frac{v}{E} = \frac{\varepsilon\zeta}{4\pi\eta} \qquad [4]$$

where U mobility of particles
ε dielectric constant
η medium viscosity (0.009 poise)
E electric field
ζ (zeta potential) is the electrostatic potential at shear plane(or the nonslip surface)

The electric field, E, can be calculated from either the voltage or current. Although the total voltage in the experiments was controlled to be constant (~40V) , because of differences in cross-sectional area, it is best to calculate E from the conductivity of the solution in which the liposomes are suspended.

From [4], the electric field was calculated from the measured current:

$$E = \frac{V}{l} = \frac{iR}{l} = \frac{i}{a\Lambda c} \qquad [5]$$

where V , i and R are voltage, current and resistance respectively. l is the electric length related to the distance between two electrodes (27). a is the cross-sectional area of the electrophoresis chamber in the viewing region (the radius of the viewing section of the chamber is 1.362 mm, given by the manufactor) and Λ is the equivalent conductivity of the solution (30). c is the concentration of the electrolyte solution.

Generally, for smooth charged particles, an assumption is made that zeta potential is equal to the potential at particle surface, $\Psi(0)$. From [2] and [3], an expression for the surface charge density is obtained (for low surface potentials):

$$\sigma = \kappa\eta U \qquad [6]$$

2.2.2 pH at Surface of the Liposomes

In aqueous systems, pH is one of the most important parameters that affect the electrostatic behaviour of the liposomes because H^+ or OH^- ions participate in the processes of ion binding to surface molecules on the liposomes.

According to the model for smooth charged particles, the concentration of any ion at the surface of liposome, C_s, is different with that of the ion in bulk solution, C_b. The relationship between these two concentrations is (27):

$$C_s = C_b \exp\left[-\frac{ZF\Psi(0)}{RT}\right] \qquad [7]$$

Considering the H^+ distribution, applying [7] and solving for $pH_s = -\log H_s^+$ gives:

$$pH_s = pH_b + \frac{F\Psi(0)}{RT} = pH_b + \frac{e\zeta}{2.303kT} \qquad [8]$$

where pH_b is the value of pH in the bulk solution (measured).

2.2.3 The Theory for "Hairy" Model Liposomes

The above relations have been widely used to describe the electrophoresis of biological cells, even though the surfaces of cells are actually more complicated than that of a smooth particle (31). The region of the glycocalyx in the real cells, as mentioned in *Section* 2.1, contains the polyelectrolyte or polymer chains which are penetrated by ions or small

electrolytes, such as carbohydrates. It causes a distribution of fixed charges throughout the glycocalyx (rather than a uniform charge distribution over the smooth surface particles) and hydrodynamic resistance produced by polymer segments.

There has been some work published which focuses on the description of the behaviour of real cells in electrophoresis (32). Levine et al. (31) offered a mathematical treatment of the cell surface, which considered the charge distribution (within the surface layer) and the hydrodynamic flow. This treatment was improved by Sharp et al. (32) and a model to represent the behaviour of liposomes bearing charged glycolipids in electrophoresis was developed by McDaniel et al (26).

The approach used to interpret the electrophoretic mobilities of liposomes containing tetra-EC or tetra-ECG is an adaptation of that described by Sharp and Brooks (32). Briefly, for particles large enough that their radius is large compared to the double layer thickness, the electrophoretic mobility is calculated from the electroosmotic velocity resulting from motion of the electrical double layer adjacent to the charged particle surface in the electric field. The resulting fluid velocity a long way from the particle surface is set equal and opposite to the particle mobility (31). For smooth particles the velocity distribution near the surface is determined only by the ion concentration profile in the double layer, increasing in magnitude with surface charge and with decreasing ionic strength. When the surface carries polymer chains which extend away from the surface into solution, however, they exert an additional drag which reduces the electroosmotic velocity and hence the mobility. At lower ionic strengths where the double layer is expanded, if the double layer, and hence the region in which electroosmosis takes place, extends beyond the surface polymer layer the effective drag associated with the chains will be reduced

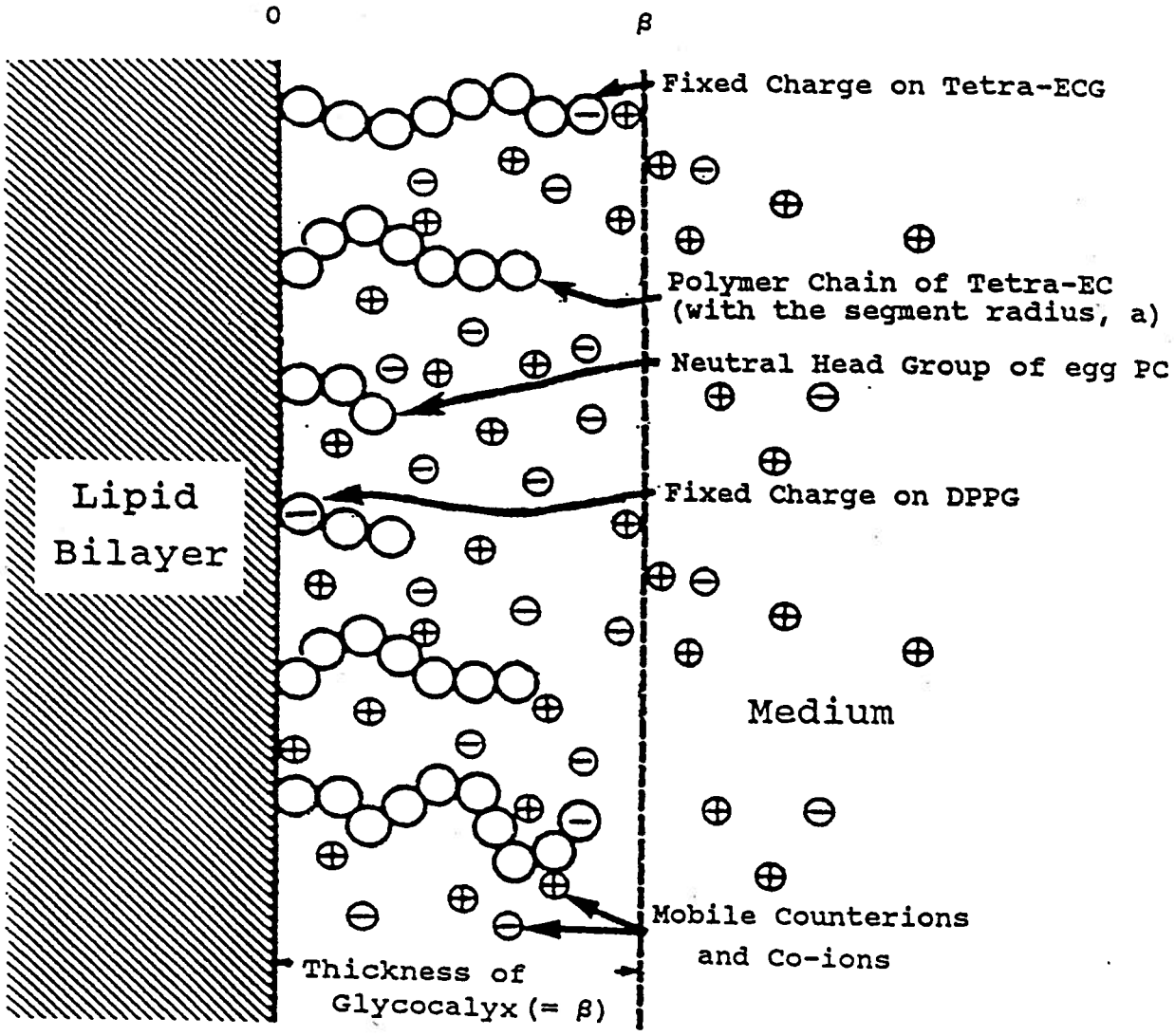

Figure 2.3 The Liposome Model of Glycocalyx

and the mobility will tend to behave more like that of a smooth particle. Hence, the ionic strength dependence is a function of the depth of the surface layer, which allows its estimation.

If the fixed surface charge is located within the region occupied by the chains the effect on the velocity profile is to reduce the overall drag relative to the case in which the charge is distributed over the smooth surface to which the polymer chains are anchored. This increases the mobility.

In the calculations utilized here, the numerical integration program described by Sharp and Brooks (32) was used. The hydrodynamic drag exerted by the polymer chains is considered to be equal to the Stokes drag exerted by segments of hydrodynamic radius a present at a uniform density throughout a thickness β. The larger the segment concentration, a or β, the greater the drag and the lower the predicted mobility. The parameters used in this program are: i) thickness of the glycocalyx, β; ii) polymer chain density (number per unit area); iii) the polymer segment radius, a (Å); iv) the fixed charge density, σ (esu/cm^2); v) the location of the fixed charge; vi) the location of the shear plane.

2.3 Methods

2.3.1 Preparation of Liposomes

Liposome behaviour and stability depend on particle size, number of bilayers, chemical composition and the composition of the aqueous phase in which liposomes are formed. It is essential to control all these factors if one is to understand the relationship between each of these properties and liposome function (33).

There have been many techniques for preparation of liposomes. The procedure (33) can be divided into three stages (*See Figure* 2.4):

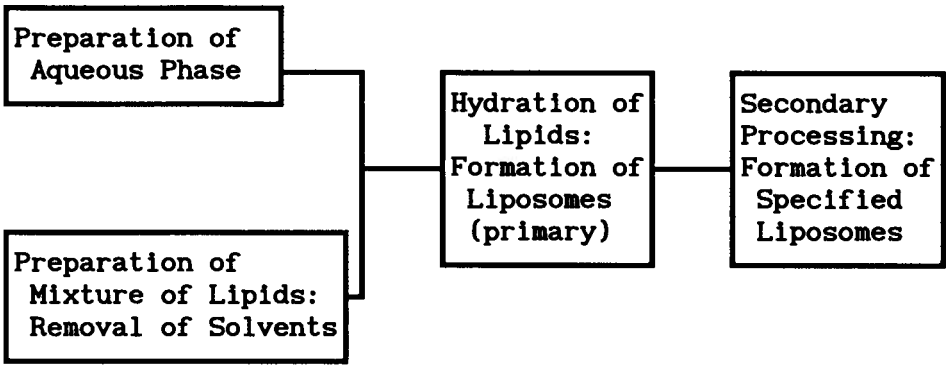

Figure 2.4 Procedure of Liposome Preparation

first, preparation of the aqueous phase and lipid mixture; second, lipid hydration and third, optional steps to make specific sorts of liposomes.

In preparation of the aqueous phase, several factors must be considered: osmolarity, ionic strength, pH, choice of materials and their concentration for both interior and exterior phases and contaminants.

For making a particular molecular mixture of lipids, each of them is first dissolved in a single or mixed solvent. Generally, all the lipids should be soluble at the desired concentrations in the chosen solvent system. A dry lipid mixture is made by removing the solvent uniformly since the form of dry lipids can seriously affect the hydration and formation of liposomes. Usually, a continuous film on the container wall is considered optimal.

The usual hydration method is to disperse the dried lipid mixture into the aqueous phase by shaking. Following this step, particular techniques

are applied for making specific liposomes, for instance of a particular size (34). In this work, however, only shaken, multilayered liposomes were used.

2.3.2 Electrophoresis Equipment

There have been many kinds of equipment used in particle electrophoresis research for various purposes. The equipment in our project was described by Seaman et al. (27) in their work on electrophoresis of red cells (*See Figure* 2.5a & 2.5b).

In *Figure* 2.5a, a constant temperature is maintained in a water bath containing a stirring device and a thermostated heater(*e*, thermostat). The calibrated vertical traverse, *b*, and the dial test indicator, *k*, provide the readings of the vertical and horizontal position of the chamber. The ocular with a fitted graticule, *h*, serves for the measurement of the distance that a particle moves in a measured interval.

The most important part in the electrophoresis apparatus is the chamber, which is mounted horizontally (between *a* and *g*); its vertical and horizontal positions are adjusted until the axis of the microscope is located at right angles and passes through the center line of the chamber.

There are two kinds of chambers, cylindrical and rectangular, which can provide accurate and reliable results. In our experiment, a cylindrical chamber similar to that described in *Figure* 2.5b was used, except that the stopcocks were replaced by plugs in ground glass joints.

The chamber can be divided functionally into two parts: the ends containing two compartments for the electrodes (in KCl solution) and the central observing section, separated by two pieces of sintered glass discs.

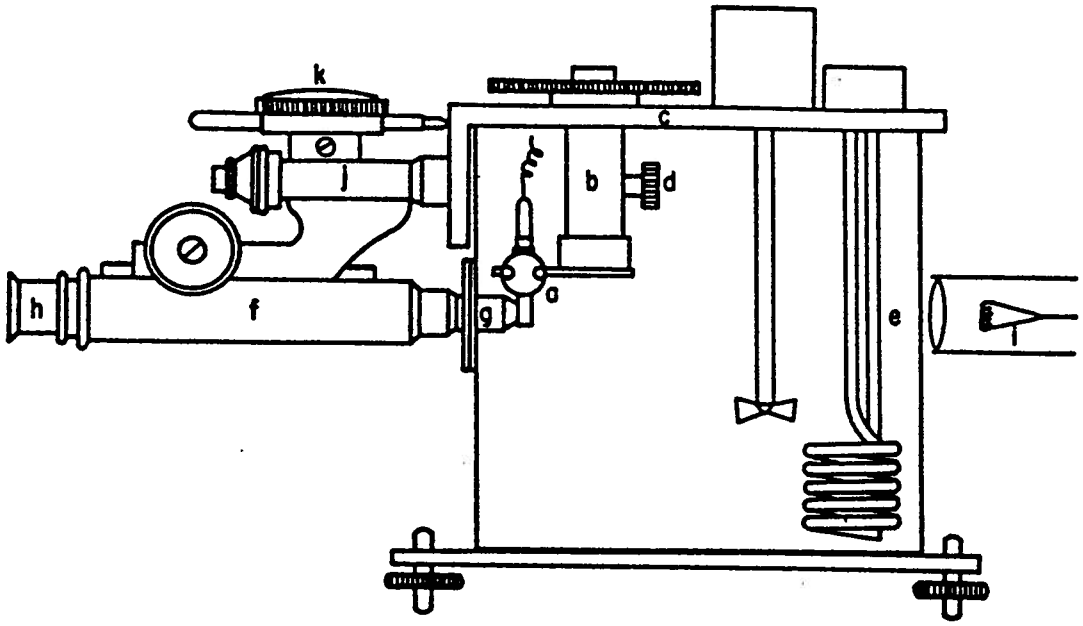

Figure 2.5a Cylindrical microelectrophoresis apparatus:

a, Tube holder; b, calibrated vertical traverse; c, crossbar; d, locking screw; e, thermostat; f, microscope tube; g,objective; h, ocular with fitted graticule/reticule; i, light source; j, microscope fine adjustment; k, dial test indicator. (27)

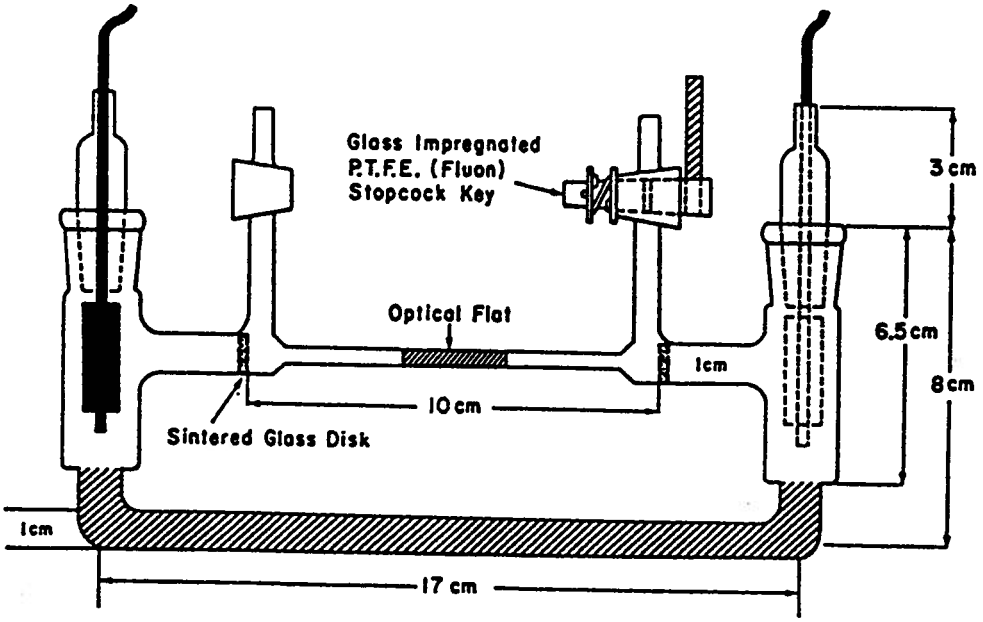

Figure 2.5b All glass small volume cylindrical electrophoresis chamber incorporating a Ag/AgCl/KCl electrode system with fused-in sintered glass discs. (27)

Current was supplied to the electrodes by a power supply operated in constant voltage mode; the voltage and current were read from two digital multimeters.

Ag/AgCl (/KCl) electrodes have been used previously and proven to be the most satisfactory system. They were treated as described in *Section* 2.4. . The refurbishing of Ag/AgCl electrode is performed with nitric acid and ammonia respectively (to recover Ag), followed by replating in a KCl solution (the detailed procedures are described in *Section* 2.4.3.1.).

2.4 Experimental

General Details

Centrifugation was carried out with a Micro Centaur Centrifuge (Johns Scientific Inc.). Solution pH was measured with an Acumet pH Meter 915 (Fisher Scientific) to $\pm$0.02 units. Current was supplied with a Hewlett Packard 6212A Power Supply; the voltage and current were read from two Hewlett Packard 3438A Digital Multimeters. The water used in preparation of aqueous solutions was from a Millipore Milli-Q Plus ultra-pure water system.

All organic solvents and reagents were used as purchased. Tetra-EC and tetra-ECG were synthesized in *Chapter* 1 (*See Section* 1.4). Particular pH solutions were made by adjusting pH prior to usage with HCl, NaOH or $NaHCO_3$ solutions of the same ionic strength as the solution being adjusted.

2.4.1 Liposome Preparation

The same procedure for preparing liposomes was used for all lipid compositions(*See Table* 2.1)

Table 2.1 Composition of Liposomes in Particle Electrophoresis

Liposome Number	Composition of Liposomes (molar ratio)				
	egg PC	DPPG	Cholesterol	tetra-EC	tetra-ECG
EL# 1	60	--	--	40	--
EL# 2	60	--	--	30	10
EL# 3	50	10	40	--	--
EL# 4	50	10	10	30	--
EL# 5	60	--	10	20	10
EL# 6	55	5	10	25	5
EL# 7-1	30	10	--	60	--
EL# 7-2	30	10	30	30	--
EL# 7-3	30	10	50	10	--
EL# 8-1	40	--	--	50	10
EL# 8-2	40	--	30	20	10
EL# 8-3	40	--	50	--	10

Sodium chloride 0.6867 g(11.75 mmol) and sodium azide (NaN_3) 0.049 g (0.75 mmol) were dissolved in a 250 ml volumetric flask as the aqueous phase for liposomes. The lipids in desired concentration were dissolved in chloroform (DPPG was warmed up to around 43°C), and transferred into a 250 ml round bottom flask (which was cleaned with chromic acid, rinsed thoroughly in water and dried prior to usage). The volume of solution was adjusted to 5 - 6 ml with chloroform. The mixture then was dried slowly with rotary evaporation under reduced pressure at room temperature. Addition of about 5 ml NaCl-NaN_3 solution was followed by incubation of the mixture in a 42°C water bath. The suspension was centrifuged for 10 to 30 minutes (13000 RPM; radius 65 mm) and the supernatant was removed. The liposomes were washed twice in 5 ml of the medium in which they were to be examined by electrophoresis. The procedure was to pipette the supernatant

carefully, resuspending the liposomes with addition of the solution of the desired pH and ionic strength, followed by centrifugation. The same resuspension and centrifugation were repeated to ensure the complete replacement by medium of the desired pH and ionic strength.

2.4.2 Electrophoresis

General Preparation(*See Figure* 2.5 for details)

All solutions were de-gassed before they were used. The cylindrical chamber was cleaned with chromic acid (CrO_3/H_2SO_4) and thoroughly rinsed before use. Ag/AgCl electrodes were washed with nitric acid and ammonia sequentially, and replated in KCl solutions at a current density of 0.43 mA/cm^2.

The water bath tank was filled and temperature was set up to be controlled at $25.00 \pm 0.02^{\circ}C$. The optical microscope was focused at the stationary level, equal to 0.293 x (radius ,1.362 mm), from the inner wall (35). At this location the fluid velocity caused by electroosmosis along the walls of the chamber is zero.

The electrode cells at both ends of the chamber were filled with KCl solution and stoppered by electrodes. (The center cell was filled with KCl solution as well when not in use.) The voltage was adjusted and controlled at nominally 40 V.

2.4.2.1 pH Dependence Studies

The experimental salt solution (NaCl 50 mM) with adjusted pH, which was also used to wash the liposomes (EL# 1 & EL# 2), was degassed and warmed in the water bath. The center chamber was filled, after being rinsed several times, with the warmed solution (*See Section* 2.3.2 & *Figure* 2.3b). One of the outlets of the center chamber was stoppered. The liposome

sample was taken in suspension in the same solution in a 1.0 ml syringe and approximately 0.1 ml injected into the viewing region ("Optical Flat") by a tubing connected to the tip of the syringe. The sample was stirred to dilute it and provide a roughly uniform distribution near the viewing region of the chamber. The other outlet was stoppered to keep the system stable during the measurement. The electric field was switched on and the motion of particles in the field was observed through the microscope at a magnification of x 320. The time taken by a particular particle to transit a fixed distance on the eyepiece graticule was recorded. The direction of the current was reversed, producing migration of the same particle in the opposite direction; the mobility of the particle was calculated from the average of the velocities which were first calculated from the pair of readings.

Usually, ten particles were observed for each pH solution and the values of voltage and current were read before and after each measurement, as well as the pH values of the NaCl solution. In the pH dependence experiments, the range from 1.8-9.9 was examined.

When an experiment was finished, the sample could be recovered with the syringe and the center chamber was washed with the next salt solution three times. For these experiments, the concentration of KCl solution in the electrode cells was kept constant (0.050 M), equal to that of NaCl in various pH solutions.

2.4.2.2 Ionic Strength Dependence Studies

The procedure for the ionic strength experiments was almost the same as the previous one, except that the concentration of KCl solution in the electrode cells was changed to be the same as that of the NaCl solution.

The ionic strength of the salt solution varied from 0.001 M to 0.100 M, with a constant pH ~ 7. The liposome samples were EL# 3 - EL# 6.

2.4.2.3 Different Compositions of Liposomes

The procedure was as described above. The salt solution was 0.050 M NaCl with pH ~ 7. The liposomes were EL# 7-1, EL# 7-2, EL# 7-3, EL# 8-1, EL# 8-2, and EL# 8-3. From EL# 7-1 to 7-3, the molar ratio of PEG chains decreased, while the charged lipid, DPPG, was held constant at 10%. From EL# 8-1 to EL# 8-3, the molar ratio of PEG chain concentration varied while the charged lipid, tetra-ECG, was held constant at 10%.

2.5 Result and Discussion

The mobility and apparent charge density of liposomes for all the experiments were calculated from the velocity data in Appendix III, with the classical theory of electrophoresis of smooth particles (*See Section* 2.2), giving *Table* 2.2, *Table* 2.3 and *Table* 2.4. The constants are given in *Section* 2.2.1. In calculations of the apparent charge densities, the equivalent conductivity Λ is given below for NaCl solution at 298°K (30):

concentration (M)	0.15	0.1	0.05	0.02	0.005	0.001
Λ ($cm^2\Omega^{-1}equiv.^{-1}$)	103.89	106.74	111.06	115.76	120.64	123.74

Table 2.2 Mobility and Charge Density with Variation of pH at Constant Ionic Strength I = 0.050 M for Liposomes EL# 1 & EL# 2 ("-" and "+" are the signs of charges)

pH (±)	Electrophoretic Mobility (μm-cm/sec-volt: ±S.D.)		Apparent Charge Density (esu/cm^2: ±S.D.)x0.001	
	Liposome #1	Liposome #2	Liposome #1	Liposome #2
9.88±0.14	-0.77±0.10	-2.23±0.09	-2.64±0.34	-7.67±0.32
9.43±0.09	-1.53±0.19	-3.36±0.19	-5.27±0.66	-11.56±0.65
7.97±0.17	-0.48±0.11	-2.40±0.24	-1.66±0.36	-8.24±0.81
7.30±0.11	0.34±0.12	-2.34±0.26	1.18±0.39	-8.05±0.90
7.03±0.05	0.07±0.07	-1.92±0.15	0.23±0.26	-6.60±0.51
6.87±0.06	0.16±0.05	-2.08±0.19	0.55±0.19	-7.15±0.67
5.99±0.02	0.24±0.15	-2.03±0.26	0.83±0.50	-6.99±0.89
4.95±0.02	0.24±0.07	-1.48±0.24	0.82±0.23	-5.07±0.82
4.91±0.02	0.23±0.03	-1.47±0.21	0.80±0.11	-5.07±0.73
3.98±0.02	0.35±0.06	-0.64±0.17	1.20±0.20	-2.18±0.60
2.97±0.02	0.60±0.07	0.17±0.09	2.07±0.24	0.58±0.29
1.90±0.02	0.80±0.05	0.74±0.06	2.75±0.16	2.55±0.21
1.89±0.03	0.88±0.04	0.82±0.09	3.01±0.15	2.83±0.32

Table 2.3 Mobility and Apparent Charge Density with Variation of Compositions at Constant pH ~ 7 and Constant Ionic Strength 0.05 M

* A and B are two measurements for one composition

Liposome	Composition (molar ratio): egg-PC/cholesterol/tetra-EC /DPPG/tetra-ECG	Electrophoretic Mobility (μm-cm/sec-volt: ±S.D.)
EL# 7-1	30 / 0 / 60 / 10 / 0	-3.47 ± 0.45
EL# 7-2A*	30 / 30 / 30 / 10 / 0	-3.46 ± 0.39
EL# 7-2B*	30 / 30 / 30 / 10 / 0	-2.93 ± 0.83
EL# 7-3	30 / 50 / 10 / 10 / 0	-3.13 ± 0.31
EL# 8-1	40 / 0 / 50 / 0 / 10	-1.53 ± 0.16
EL# 8-2	40 / 30 / 20 / 0 / 10	-1.85 ± 0.02
EL# 8-3	40 / 50 / 0 / 0 / 10	-2.29 ± 0.11

Table 2.4 Mobility and Apparent Charge Density
with Variation of Ionic Strength
at Constant pH around 7 for Liposomes #3,4,5 & 6

* repeated measurement

Ionic Strength (M)	Electrophoretic Mobility (μm-cm/sec-volt: ±S.D.)		Apparent Charge Density (esu/cm^2: S.D.)x0.001	
	Liposome #3	Liposome #4	Liposome #3	Liposome #4
0.001	-4.39±0.40	-3.78±0.40	-1.23±0.11	-1.06±0.11
0.005	-2.85±0.32	-2.14±0.31	-1.79±0.20	-1.34±0.19
0.005*	-3.58±0.33	-3.14±0.38	-2.24±0.21	-1.97±0.24
0.020	-3.13±0.26	-1.78±0.19	-3.92±0.33	-2.23±0.23
0.050	-2.71±0.20	-1.20±0.19	-5.37±0.41	-2.39±0.38
0.100	-1.55±0.27	-0.91±0.14	-4.35±0.77	-2.56±0.39
Ionic Strength (M)	Electrophoretic Mobility (μm-cm/sec-volt: ±S.D.)		Apparent Charge Density (esu/cm^2: S.D.)x0.001	
	Liposome #5	Liposome #6	Liposome #5	Liposome #6
0.001	-3.79±0.16	-4.11±0.18	-1.06±0.04	-1.15±0.05
0.005	-3.50±0.13	-3.54±0.35	-2.20±0.08	-2.22±0.22
0.005*	-3.27±0.18	-3.67±0.25	-2.05±0.11	-2.30±0.16
0.020	-3.27±0.16	-2.71±0.14	-4.10±0.20	-3.40±0.17
0.050	-2.65±0.19	-2.11±0.15	-5.25±0.38	-4.18±0.31
0.100	-1.90±0.18	-1.60±0.45	-5.33±0.52	-4.49±1.26

2.5.1 pH Dependence

Since the liposome #2 (EL# 2) has the composition of tetra-ECG instead of tetra-EC in the liposome #1 (EL# 1), the mobility should differ due to the presence of PEG chains and the location of the charges, even though the net charge density is expected to be the same.

From *Table* 2.2, a phenomenon was observed that EL#1 with a neutral surface had low mobilities in all the pH range, because the surface of liposomes can adsorb ions which are concentrated in solution by van der Waals interactions. The net charge density was calculated with deduction of the results of EL# 1 from those of EL# 2.(*See* Table 2.5)

Table 2.5 Calculation of Net Electrophoretic Mobility, Net Charge Density of Liposome #2 and pH at Surface of Liposomes with Variation of pH at Constant I = 0.050 M for Charged Liposome EL# 2 ($\sigma' = \sigma_2 - \sigma_1$)

pH (measured)	Electrophoretic Mobility U' = U2 - U1 (μm-cm/sec-volt: ±S.D.)	Net Surface Charge Density (esu/cm^2)x 0.001	pH at surface of liposome
9.88±0.14	-1.46 ± 0.14	-5.03 ± 0.47	9.56±0.14
9.43±0.09	-1.83 ± 0.27	-6.28 ± 0.93	9.03±0.10
7.97±0.17	-1.92 ± 0.26	-6.59 ± 0.89	7.55±0.18
7.30±0.11	-2.69 ± 0.29	-9.23 ± 0.98	6.71±0.13
7.03±0.05	-1.99 ± 0.17	-6.83 ± 0.57	6.59±0.06
6.87±0.06	-2.24 ± 0.20	-7.70 ± 0.70	6.38±0.07
5.99±0.02	-2.27 ± 0.30	-7.82 ± 1.02	5.49±0.07
4.95±0.02	-1.72 ± 0.25	-5.90 ± 0.85	4.57±0.06
4.91±0.02	-1.71 ± 0.21	-5.87 ± 0.73	4.54±0.05
3.98±0.02	-0.99 ± 0.18	-3.38 ± 0.63	3.76±0.04
2.97±0.02	-0.44 ± 0.11	-1.50 ± 0.38	2.87±0.03
1.90±0.02	-0.06 ± 0.08	-0.29 ± 0.27	1.89±0.03
1.89±0.03	-0.05 ± 0.10	-0.18 ± 0.35	1.88±0.04

Theoretically, the surface charge density of liposome #2 is constant and can be calculated from its lipid composition. The surface charge density is expressed as the net charge on the surface divided by the surface area. The composition of EL# 2 is known as 60% egg PC, 30% tetra-EC and 10% tetra-ECG. The surface area occupied per molecule of egg PC was estimated by De Young et al. (36) as 50 $Å^2$(in presence of 40% cholesterol). With the assumption that the surface area taken per lipid for tetra-EC or tetra-ECG is the same as that of cholesterol, which was reported to be 37 $Å^2$ (36), the surface charge density was calculated to be 1.07×10^4 esu/cm^2. It is obvious from *Table* 2.2 that the results

calculated from electrophoresis were lower than this estimate.

The pH at the particle surface was calculated with the classical theory and the mobilities of the liposome particles were plotted as a function of surface pH (*see Table* 2.5 & *Figure* 2.6).

The pK_a of the charged liposome, which is also the pK_a of the charged lipid (tetra-ECG), calculated from *Figure* 2.6, was equal to 3.9.

2.5.2 Composition Dependence

Two groups of liposomes, with variation of PEG chain density at the surface of the particles, were observed. The plot of the mobility vs the molar percentage of PEG chains in each liposome is given in *Figure* 2.7.

In the liposomes #7-1, 7-2 and 7-3, the negative charge was contributed from 10% (molar) DPPG and located on the surface of the bilayer. The mobilities can be considered unchanged within the experimental error when the PEG chain density was varied.

In the results of the liposomes #8-1, 8-2 and 8-3, the mobility slightly decreased while the PEG chain concentration increased.(The charge, contributed from tetra-ECG in these liposomes was located at the outer plane of the glycocalyx.) This is the usual case when the polymer chain density increases. The resistance of the motion of liposomes increases, causing mobility to decrease; while the charge density is kept constant.

For the liposomes #7-1, 7-2 and 7-3 (with constant 10% DPPG), however, the mobility was almost unchanged while the PEG chain density increased.

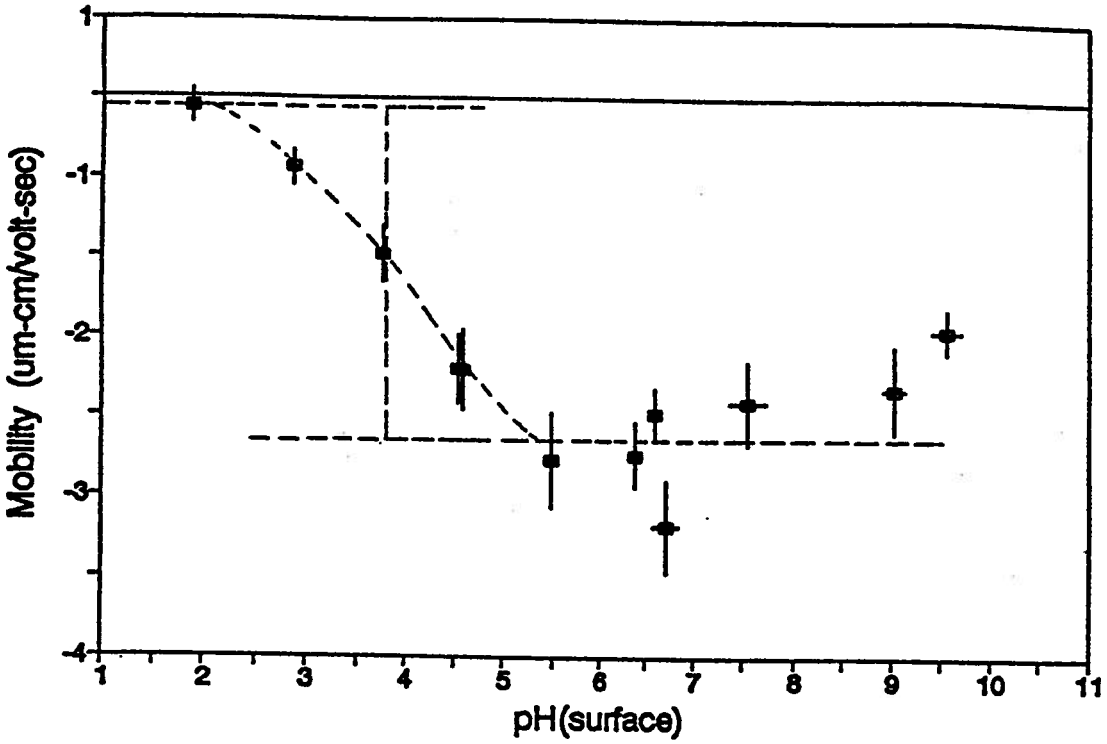

Figure 2.6 Net Liposome Mobility *vs* pH at Surface of Liposomes for EL#2 at constant ionic strength 0.050 M

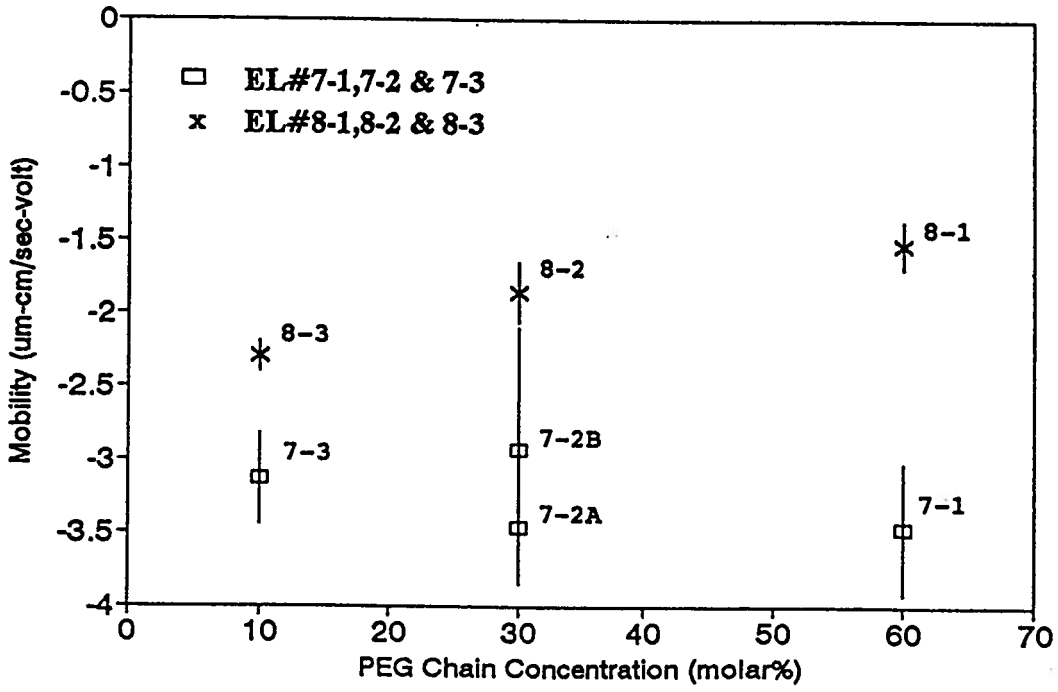

Figure 2.7 Electrophoretic Mobility *vs* PEG Chain Concentration for Different Compositions at ionic strength 0.050 M and pH ~ 7

2.5.3 Ionic Strength Dependence

The mobilities of the liposomes EL# 3, EL# 4, EL# 5 & EL# 6 are plotted as a function of ionic strength in *Figure* 2.8.

EL#3 and EL#4 have the same charge locations (DPPG, inner plane) and charge density, but different PEG chain concentrations. The EL#3 particle, which has lower PEG chain density, moves more quickly in the electric field than EL#4 at all ionic strengths.

EL#4, EL#5 and EL#6 have the same PEG chain density and charge density, but different charge locations. The mobilities of EL#6 are between those of EL#4 and EL#5 at high ionic strength, as expected since the charges in EL#4, EL#5 and EL#6 are distributed at the inner plane, outer plane and both positions, respectively. At low ionic strength, the mobilities are almost the same within experimental error.

The numerical model was used to fit the data. The results are listed in *Table* 2.6 and the figures with a more detailed description of the fitting procedure in Appendix IV.

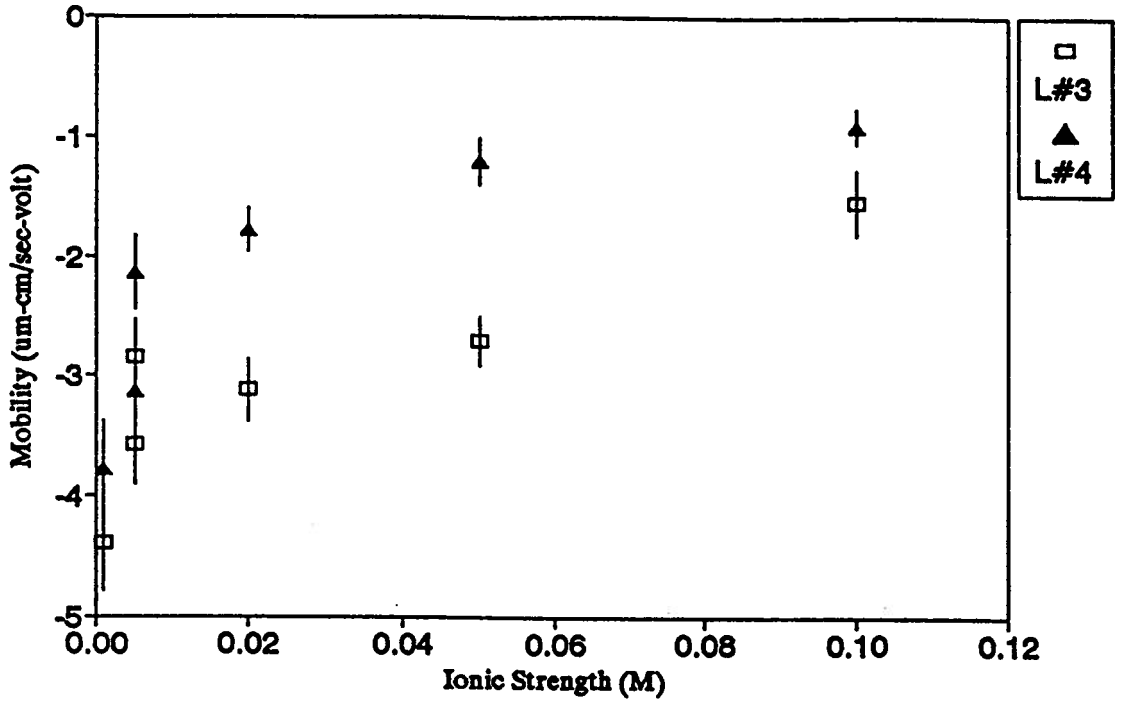

Figure 2.8a Electrophoretic Mobility *vs* Ionic Strength for EL#3 and #4 at constant pH ~ 7

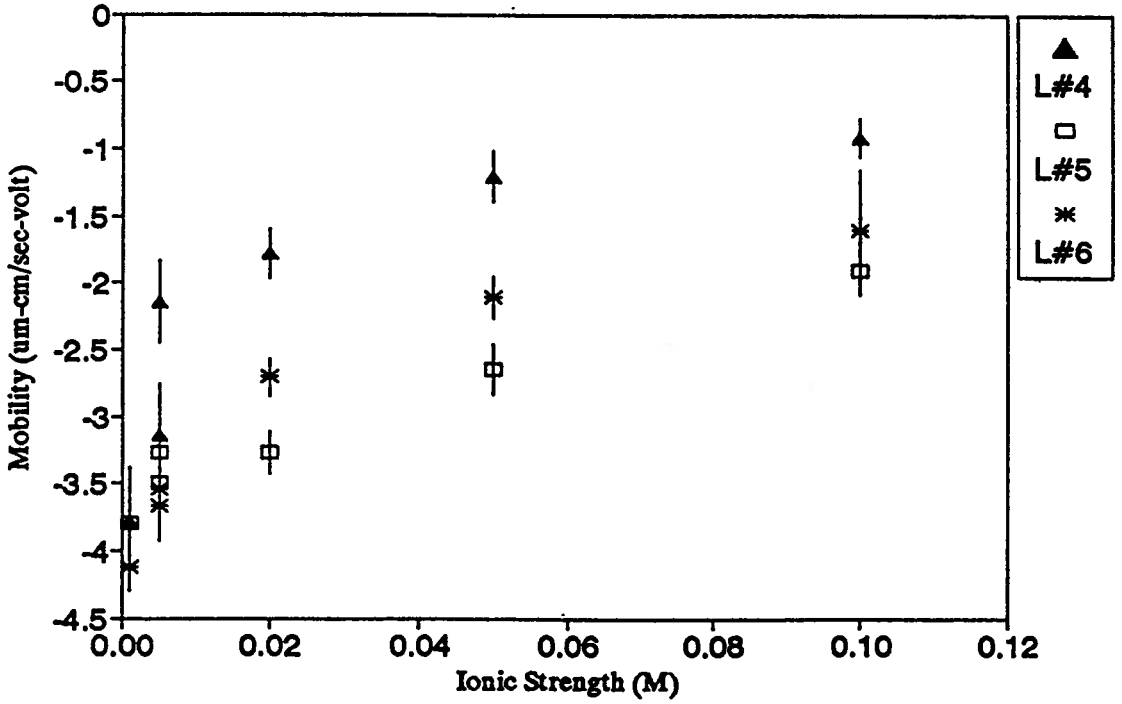

Figure 2.8b Electrophoretic Mobility *vs* Ionic Strength for EL#4, #5 and #6 at constant pH ~ 7

Table 2.6 Comparison of Mobility Model Parameters for Four Liposome Preparation (EL#3,4,5 & 6)

Preparation	Ionic Strength (mM)	Charge Density (esu/cm^2)	Molecular Density ($molec./cm^2$)	Extension (Å)
EL#3:				
CHEMICAL				
DPPG 10%		10700	2.2E+13	8
egg PC 50%			1.1E+14	8
MOBILITY	>10	8500	1.3E+14	8
	<10	8500	1.3E+14	>8
EL#4:				
CHEMICAL				
DPPG 10%		10700	2.2E+13	8
egg PC 50%			1.1E+14	8
tetra-EC 30%			6.6E+13	15
MOBILITY	1-150	9500	1.3E+14	8
			6.6E+13	15-73
EL#5:				
CHEMICAL				
egg PC 60%			1.3E+14	8
tetra-EC 20%			4.4E+13	15
tetra-ECG 10%		10700	2.2E+13	21
MOBILITY	>10	5750	2.2E+13	21
			4.4E+13	15
	<10	<5000	2.2E+13	21
			4.4E+13	15
EL#6:				
CHEMICAL				
DPPG 5%		5350	1.1E+13	8
egg PC 55%			1.2E+14	8
tetra-EC 25%			5.5E+13	15
tetra-ECG 5%		5350	1.1E+13	21
MOBILITY	>10	4250	6.2E+13	15
		2875	2.2E+14	21

2.6 Conclusion

Tetraethoxycholesterol and tetra-EC terminated with glucuronic acid, tetra-ECG, were successfully synthesized and purified in sufficient yield to allow their investigation in model membranes. A series of liposomes composed of egg PC, DPPG, cholesterol, tetra-EC and tetra-ECG were made and observed with particle electrophoresis. The pKa of tetra-ECG was estimated to be 3.9 from the pH dependence of tetra-ECG-containing liposomes, taking into account the difference in pH between the surface region and the bulk phase when the surface is negatively charged.

The electrophoretic mobilities of the liposomes were measured as a function of ionic strength of the suspending medium. The classical theory for smooth particles was found not to describe the data, particularly when PEG chains were anchored in the surface. The model of Sharp and Brooks was found to be more successful in describing the general effects of tetra-EC and tetra-ECG, allowing the experimental data to be fit with physically reasonable parameter values for chain extension and charge density at ionic strengths above 10 mM. The data taken at low ionic strengths did not fit either theory in the presence or absence of surface polymer chains, however, suggesting that the surface charge density was not constant under these conditions, possibly due to the adsorption phenomena.

REFERENCES

1. Jain, M.K., Nonrandom Lateral Organization in Bilayers and Biomembranes, in Membrane Fluidity in the Biology Vol.1, ed. Aloia, R.C., Academic Press, New York, 1983

2. Cullis, P.R., Hope, M.J., Physical Properties and Functional Roles of Lipids in Membranes, in Biochemistry of Lipids and Membranes , ed. Vance, D.E., Vance, J.E., 1992

3. Gorter, E., Grendel, F., *Journal of Experimental Medicine*, 41, 439-443pp, 1925

4. Singer, S.J., Nicolson, G.L., *Science*, 175, 720-730pp, 1972

5. Brockerhoff, H., Molecular Designs of Membrane Lipids, in Bioorganic Chemistry, 1pp, 1977

6. Ponpipom, M.M., Shen, T.Y., Baldeschwieler, J.D., Wu, P.-S., Liposome Technology, Vol. III, 95-115pp, 19

7. Sather, P.J., "Synthesis of Cholesterol Based Model Glycolipids", Master Thesis, The University of British Columbia, Canada, 1990

8. (a)Kunitake, T., Okahata, Y., *Bulletin of Chemical Society of Japan*, Vol.51(6), 1877-1879pp, 1978
   (b)Farhood, H., Bottega, R., Epand, R.M., Huang, L., *Biochimica et Biophysica Acta*, 1111, 239-246pp, 1992

9. Demel, R.A., De Kruyff, B., *Biochimica et Biophysica Acta*, 457, 109-132pp, 1976

10. Johnston, D.S., Coppard, E., Parera, G.V., Chapman, D., *Biochemistry*, 23, 6912-6919pp, 1984

11. Crowe, J.H., Crowe, L.M., Carpenter, J.F., Rudolph, A.S., Wistrom, C.A., Spargo, B.J., Anchordoguy, T.J., *Biochimica et Biophysica Acta*, 974(2), 367-384pp, 1988

12. Chandrasekhar, I., Gaber, B.P., *Journal of Biomolecular Structure & Dynamics*, Vol.5, 1163-1171pp, 1988

13. Harris, J.M., Introduction to Biotechnical and Biomedical Applications of Poly(ethylene glycol), in Poly(Ethylene Glycol) Chemistry: Biotechnical and Biomedical Applications, ed. Harris, J.M., Pleum, New York,1992

14. Brockerhoff, H., Ramsammy, L.S., *Biochimica et Biophysica Acta*, 691, 227-232pp, 1982

15. Patel, K.R., Li, M.P., Schuh, J.R., Baldeschwieler, J.D., *Biochimica et Biophysica Acta*, 797, 20-26pp, 1984

16. Patel, K.R., Li, M.P., Schuh, J.R., Baldeschwieler, J.D., *Biochimica et Biophysica Acta*, 814, 256-264pp, 1985

17. Bollenback, G.N., Long, J.W., Benjamin, D.G., Lindquist, J.A., *Journal of the American Chemical Society*, 77, 3310pp, 1955

18. Paudler, W.W., Nuclear Magnetic Resonance, *Chapter* 3, Allyn and Bacon, Boston, 1971

19. Goodrich, R.P., Crowe, J.H., Crowe, L.M., Baldeschwieler, J.D., *Biochemistry*, 30, 5313-5318pp, 1991

20. Schneider, J.J., Bhacca, N.S., *Journal of Organic Chemistry*, 34(6), 1990-1993pp, 1969

21. Goodrich, R.P., Handel, T.M., Baldeschwieler, J.D., *Biochimica et Biophysica Acta*, 938, 143-154pp, 1988

22. Pathak, V.P., *Synthetic Communications*, 23(1), 83-85pp, 1993

23. (a)Wu, S.-H., Ong, G.-T., Hsiao, K.-F., Wang, K.-T., *Journal of the Chinese Chemical Society*, 39, 675-682pp, 1992
(b)Chang, K.-Y., Wu, S.-H., Wang, K.-T., *Carbohydrate Research*, 222, 121pp, 1991

24. Bangham, A.D., Liposomes: An Historical Perspective, in Liposomes, ed. Ostro, M.J., 1-26pp, Marcel Deckker Inc., New York, 1983

25. Juliano, R.L., Interaction of Proteins and Drugs with Liposomes, in Liposomes, ed. Ostro, M.J., Marcel Dekker Inc., New York, 1983

26. McDaniel, R.V., Sharp, K., Brooks, D.E., McLaughlin, A.C., Winiski, A.P., Cafiso, D., MaLaughlin, S., *Biophysical J.*, 49, 741-752pp, 1986

27. Seaman, G.V., Electrokinetics Behavior of Red Cells, in The Red Blood Cell, Vol.2, ed. Surgenor, D.M., Academic Press, New York, 1975

28. Popiel, W.J., Introduction to Colloid Science, *Chapter* 9, 152pp, Exposition Press, New York, 1978

29. Davies, J.T., Rideal, E.K., Interfacial Phenomena, *Chapter* 2, 75pp, Academic Press, London, 1963

30. Robinson, R.A., Stokes, R.H., Electrolyte Solutions, 41-45pp & 465-466pp, Butterworth, London, 1959

31. Levine, S., Levine, M., Sharp, K.A., Brooks, D.E., *Biophysical Journal*, 42, 127-135pp, 1983

32. Sharp, K.A., Brooks, D.E., *Biophysical Journal*, 47, 563-566pp, 1985

33. Woodle, M.C., Papahadjopoulos, D., Liposome Preparation and Size Characterization, in Methods in Enzymology, Vol.171, ed. Colowick, S.P., Kaplan, N.O., 1989

34. Jousma, H., Talsma, H., Spies, F., Joosten, J.G.H., Junginger, H.E., Crommelin, D.J.A., *International Journal of Pharmaceutics*, 35, 263-274pp, 1987

35. From personal communication with Robert J. Knox, Western Biomedical Research Institute, P.O.Box 22510, Eugene, Oregon 97402-0419

36. De Young, L.R., Dill, K.A., *Biochemistry*, 27, 5281-5289pp, 1988

LIST OF APPENDICES

Appendix I Molecular Model of Tetra-ECG

(Builded and studied with INSIGHT II Modeling System)

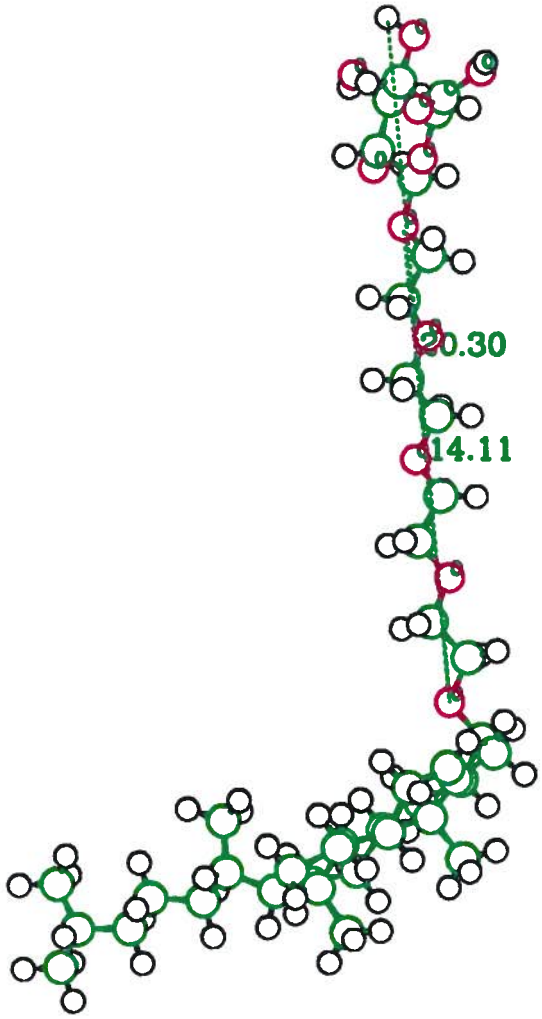

A1

Appendix II (a) ^{1}H NMR Analysis of Brominated and Protected Sugar(2)

Part of the whole spectrum of proton NMR 400 MHz is shown with the chemical shift varying from 4.3 to 7.3 ppm. The single peak around 7.2 is from the solvent deuterium chloroform. The signals at 4.57, 4.84, 5.22, 5.59 and 6.62 ppm refer to H5, H2, H4, H3 and H1 respectively. The coupling constant of H1 and H2, J_{12}, is measured and calculated to be 4 Hz, smaller than that of the axial-axial coupling, 9-14 Hz (17); while J_{23}, J_{34} and J_{45} are the same 11Hz.

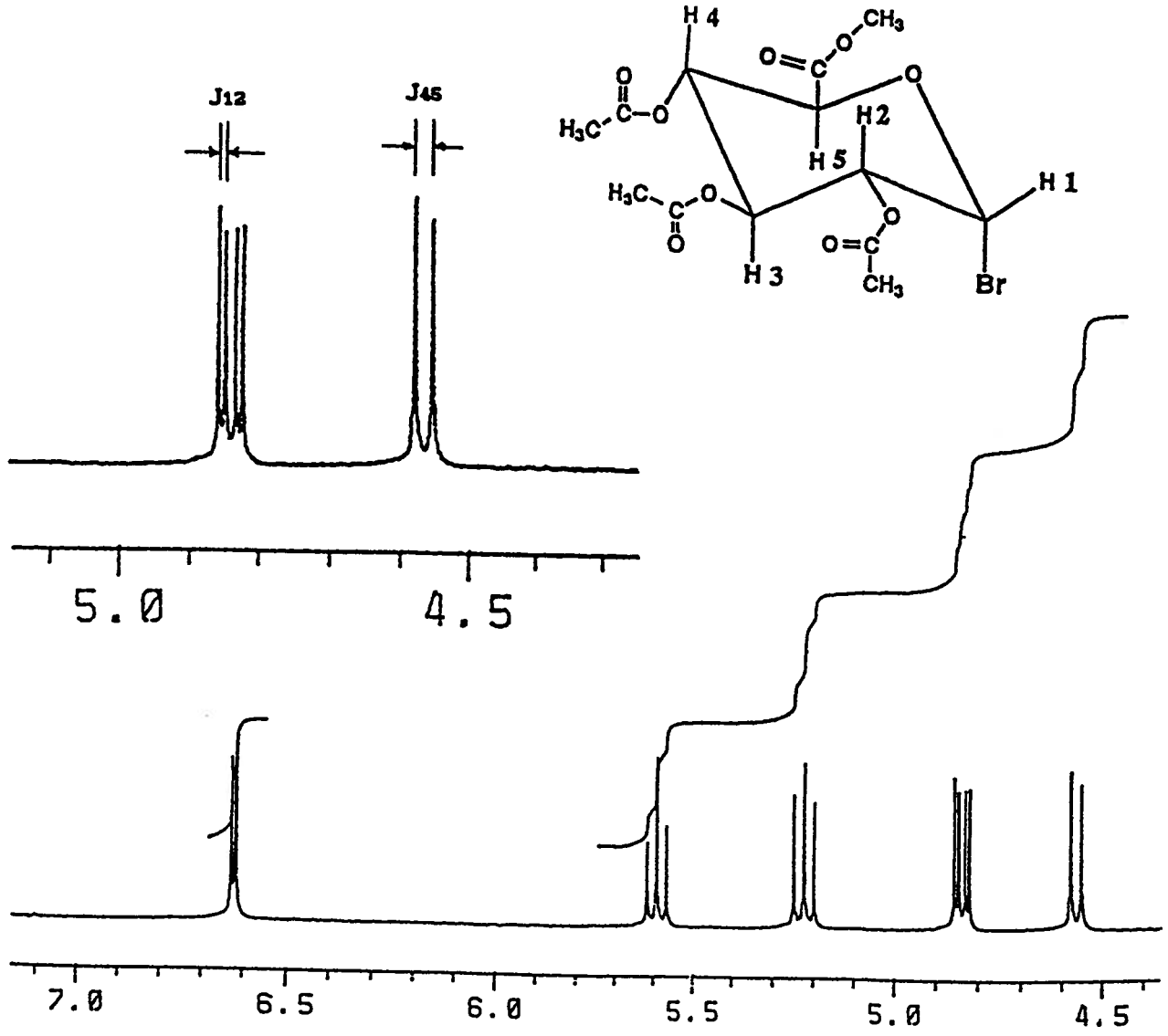

Appendix II (b) ^{1}H NMR Analysis of the Compounds in Coupling Reaction

The estimation of the molar ratio of tetra-EC and tetra-ECPG is based on the assumption that the mixture only composes of these two compounds. At the left below a table shows whether or not and which proton(s) of tetra-EC or tetra-ECPG contribute to the NMR integral of a particular signal.

Chemical Shift(ppm)	tetra-EC	tetra-ECPG
0.4-2.6	44Hc	44Hc+9Ha
~3,2	1Ho	---
3.4-4.5	16Hp	16Hp+3Hm+1Hs
4.5-5.6	1Hcd	4Hs+1Hcd

a acetyl group c cholesterol
cd double bond in cholesterol
m methyl group on sugar part
o hydroxyl group
p PEG chain s sugar ring

Assume the molar ratio of tetra-EC and tetra-ECPG is $\chi_1 : \chi_2$. Assign the relations as:

$$44\chi_1 + 53\chi_2 = \text{ITGL 1}$$
$$\chi_1 = \text{ITGL 2}$$
$$16\chi_1 + 20\chi_2 = \text{ITGL 3}$$
$$\chi_1 + 5\chi_2 = \text{ITGL 4}$$

The ratio $\chi_1 : \chi_2$ can be given by any two of these equations.

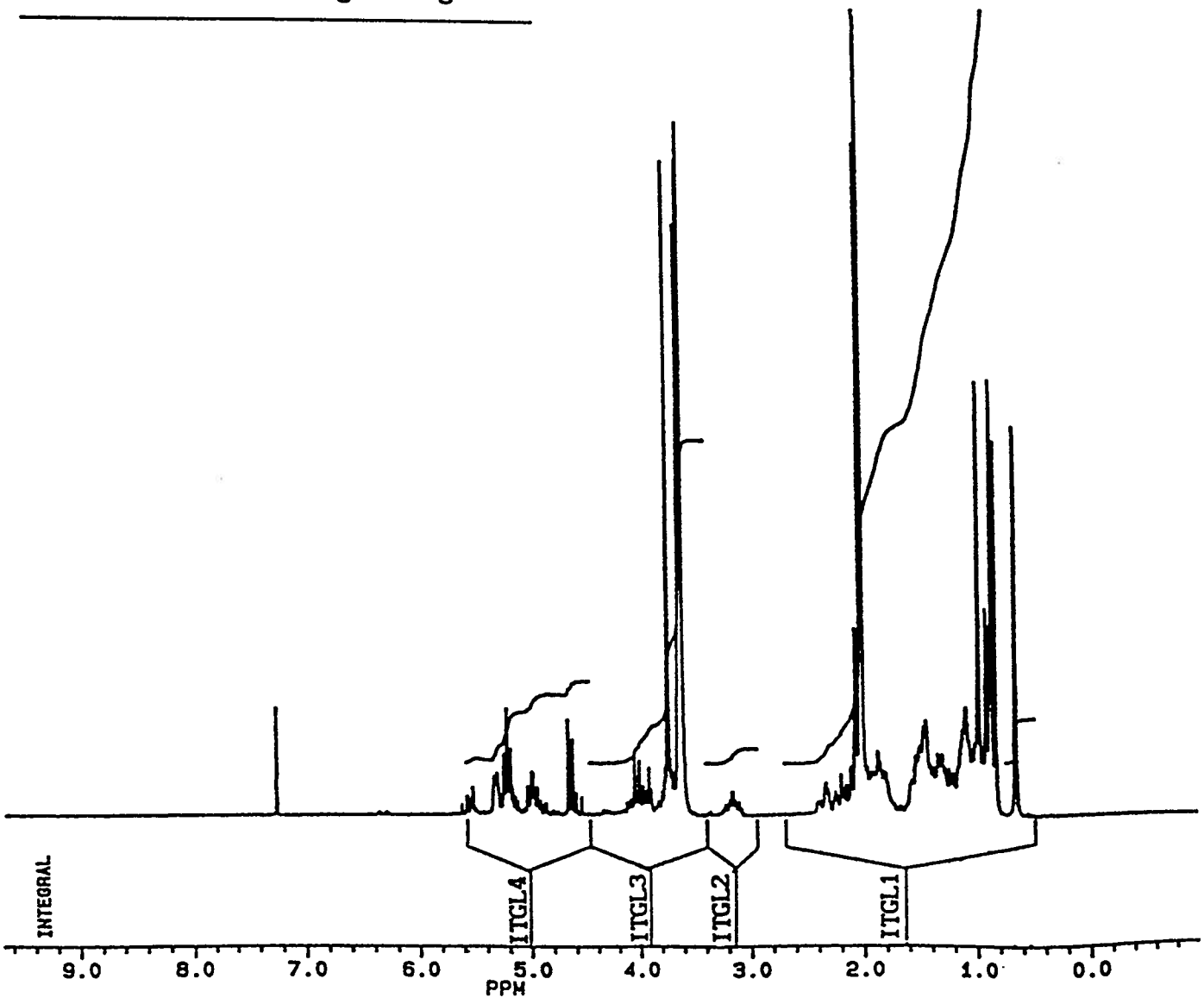

Appendix II (c) 200 MHz ^{1}H NMR Analysis of Deprotected Compound (6)

Chemical Shift(ppm)	Integral/Ratio	tetra-ECG
0.4-2.6	412.7/45.9	44Hc
3.0-4.8	217.4/24.2	16Hp+3Ho+5Hs
~5.4	9.00/1	1Hcd

c cholesterol s sugar ring
cd double bond in cholesterol
o hydroxy group p PEG chain

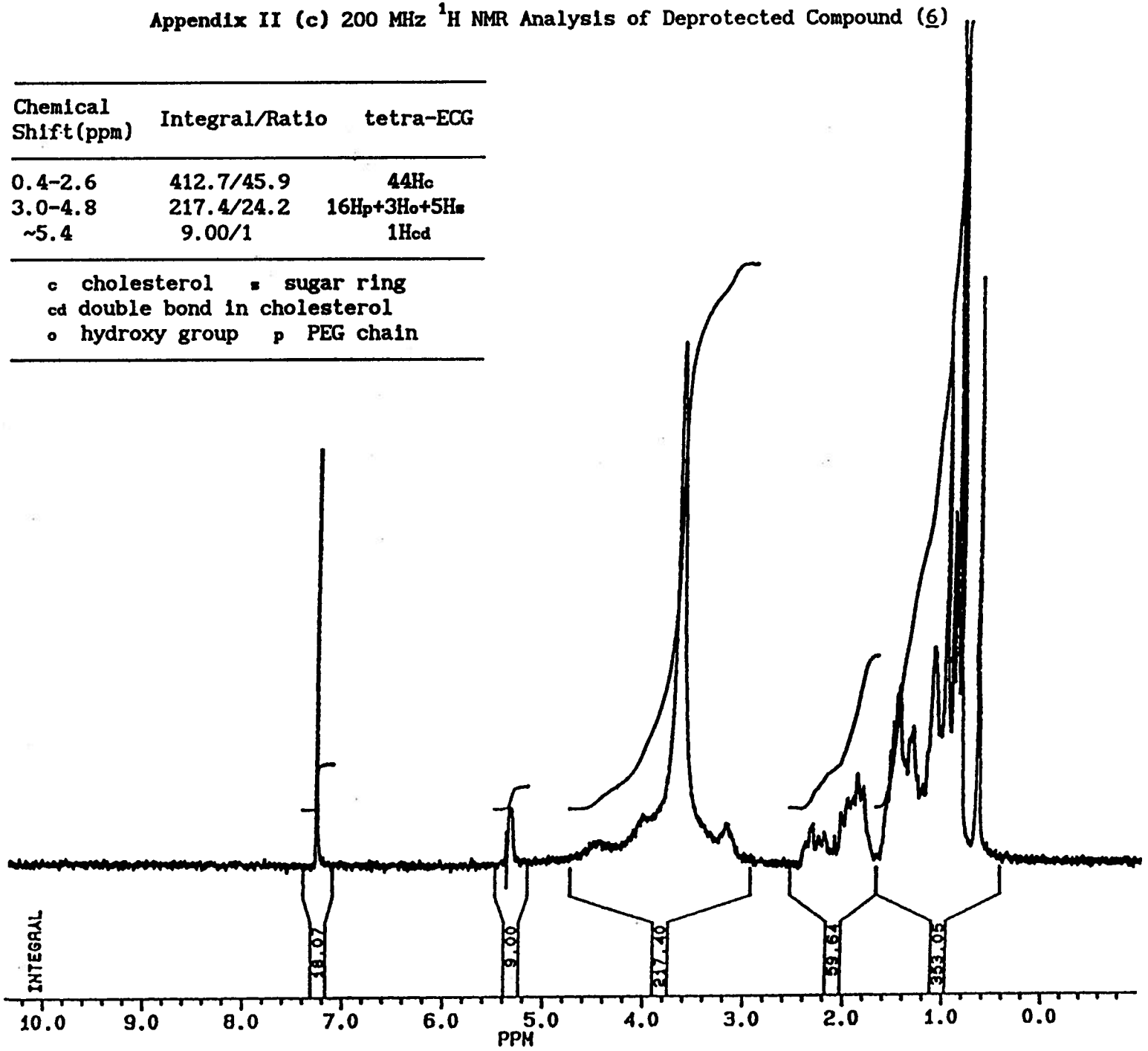

Appendix III Particle Velosity Data Tables

Velosity of liposome particle is: $v = d/t = \frac{nD}{t}$

where d is the distance the particle moves in particular time; D is the length per division, 0.024mm; n is the number of division.

The average velosity is obtained from the average of the inversions of all the time readings from motion of different particles, multiplied by d.

Liposome # 1 (EL# 1) (constant ionic strength at 0.050M)

pH (±)	Charge Sign (+/-)	Average Velosity (cm/sec: ± S.D.) x 10000	Current (mA)	Voltage (V)
9.88 ± 0.14	-	-2.63 ± 0.34	1.11	40.01
9.43 ± 0.09	-	-5.26 ± 0.66	1.11	39.91
7.97 ± 0.17	-	-1.67 ± 0.37	1.12	40.00
7.30 ± 0.11	+	1.12 ± 0.47	1.10	39.91
7.03 ± 0.05	+	0.23 ± 0.26	1.12	40.01
6.87 ± 0.06	+	0.55 ± 0.19	1.11	40.02
5.99 ± 0.02	+	0.80 ± 0.52	1.11	40.01
4.95 ± 0.02	+	0.82 ± 0.23	1.11	40.01
4.91 ± 0.02	+	0.81 ± 0.11	1.12	40.02
3.98 ± 0.02	+	1.21 ± 0.20	1.12	40.01
2.97 ± 0.02	+	2.19 ± 0.25	1.18	39.98
1.90 ± 0.02	+	4.63 ± 0.28	1.87	39.91
1.89 ± 0.03	+	5.12 ± 0.25	1.89	40.00

Liposome # 2 (EL# 2) (constant ionic strength at 0.050M)

pH (±)	Charge Sign (+/-)	Average Velosity (cm/sec: ± S.D.) x 10000	Current (mA)	Voltage (V)
9.88 ± 0.14	-	-7.66 ± 0.32	1.11	40.00
9.43 ± 0.09	-	-11.53 ± 0.65	1.11	39.91
7.97 ± 0.17	-	-8.23 ± 0.81	1.11	40.00
7.30 ± 0.11	-	-7.94 ± 0.88	1.10	39.95
7.03 ± 0.05	-	-6.58 ± 0.51	1.12	40.02
6.87 ± 0.06	-	-7.14 ± 0.67	1.11	40.02
5.99 ± 0.02	-	-6.98 ± 0.87	1.11	40.02
4.95 ± 0.02	-	-5.06 ± 0.82	1.11	40.02
4.91 ± 0.02	-	-5.08 ± 0.73	1.12	40.01
3.98 ± 0.02	-	-2.20 ± 0.63	1.12	40.01
2.97 ± 0.02	+	0.61 ± 0.31	1.18	39.99
1.90 ± 0.02	+	4.31 ± 0.36	1.88	39.91
1.89 ± 0.03	+	4.80 ± 0.53	1.89	40.00

Appendix III Particle Velosity Data Tables

Liposome #3 (EL# 3) (constant pH)

Ionic Strength (M)	pH (±0.02)	Average Velosity (cm/sec: S.D.) x 10000	Current (mA)	Voltage (mV)
0.005	6.94	-15.00 ± 1.37	0.127	39.82
0.020	6.91	-11.89 ± 0.99	0.461	39.89
0.050	6.88	- 9.27 ± 0.70	1.11	39.90
0.100	6.95	- 5.36 ± 0.94	2.10	39.94

Liposome #4 (EL# 4) (constant pH)

Ionic Strength (M)	pH (±0.02)	Average Velosity (cm/sec: S.D.) x 10000	Current (mA)	Voltage (mV)
0.005	6.94	-13.16 ± 1.60	0.127	39.84
0.020	6.91	- 6.77 ± 0.70	0.462	39.91
0.050	6.88	- 4.12 ± 0.65	1.11	39.92
0.100	6.95	- 3.81 ± 0.49	2.11	39.95

Liposome #5 (EL# 5) (constant pH)

Ionic Strength (M)	pH (±0.02)	Average Velosity (cm/sec: S.D.) x 10000	Current (mA)	Voltage (mV)
0.005	6.97	-15.03 ± 0.56	0.130	39.99
0.020	6.91	-12.51 ± 0.60	0.464	39.99
0.050	6.88	- 9.08 ± 0.65	1.11	39.93
0.100	6.95	- 6.57 ± 0.63	2.10	39.93

Liposome #6 (EL# 6) (constant pH)

Ionic Strength (M)	pH (±0.02)	Average Velosity (cm/sec: S.D.) x 10000	Current (mA)	Voltage (mV)
0.005	6.94	-15.40 ± 1.06	0.127	39.84
0.020	6.91	-10.34 ± 0.52	0.463	39.97
0.050	6.88	- 7.24 ± 0.53	1.11	39.94
0.100	6.95	- 5.59 ± 1.56	2.12	39.99

Appendix III Particle Velosity Data Tables

Velosity of Electrophoresis for

Liposome Composition Dependence

(constant pH and ionic strength)

Liposome with different composition	Average Velosity (cm/sec: S.D.) x 10000	Current (mA)	Voltage (mV)
EL# 7-1	-11.79 ± 1.54	1.10	40.00
EL# 7-2A*	-11.76 ± 1.31	1.10	39.91
EL# 7-2B*	- 9.97 ± 2.82	1.10	39.92
EL# 7-3	-10.65 ± 2.19	1.10	39.89
EL# 8-1	- 5.19 ± 0.54	1.10	39.93
EL# 8-2	- 6.31 ± 0.69	1.10	39.93
EL# 8-3	- 7.79 ± 0.36	1.10	39.92

PH 6.96 ± 0.02, Ionic Strength 0.050 M

* A & B are two measurements for composition EL# 7-2

Appendix IV Data Fit to Equations for Mobilities of Hairy Particles

Contributed by X. Song, J. Janzen and D. E. Brooks

Model Parameters

The mobility model assumes a region, the glycocalyx, exterior to the bilayer which contains surface associated molecules and suspending medium. Some of these associated molecules bear charged groups. The mobility is calculated as a function of the ionic strength of the suspending medium.

The composition data for the liposomes and structural data for the molecular species were used to calculate parameter values which were expected to fit the mobility data. The parameter values were then varied to improve the fit. Assessment of the degree of fit was qualitative.

The mole percent data for the liposome components were first converted into molecular surface densities, i.e., molecules/cm^2. This calculation used the reported areas per molecule for egg PC (50 $Å^2$) and cholesterol (37 $Å^2$) in 40 mole % cholesterol bilayers (36). Surface charge densities were calculated from molecular densities assuming one ionized group per carboxylic acid and phosphodiester residue. Ten mole percent of a species with a single charge per molecule corresponds to 2.2×10^{13} molecules/cm^2 and 10700 esu/cm^2.

In the mobility calculation the electrostatic charge density contributes a positive term to the magnitude of the particle mobility while the interaction of anchored molecular chains with the suspending medium is resistive. In the current program, electrostatic charge may be specified independently at the inner and outer interfaces of the glycocalyx and as a

diffuse charge within the glycocalyx. In the latter case the volume density of the charge is calculated from the surface charge density and either a gaussian distribution function or a uniform distribution function. Diffuse charge distributions were not used in these calculations.

Stokes resistance is characterized by a radius which is estimated here from structural data. In reality this parameter is a hydrodynamic characteristic. This parameter is referred to here as the segment radius and was set equal to one-half the unit cell length of the head group chain of tetraethoxycholesterol (tetra-EC), 1.85 Å.

The resistive term varies with distance from the bilayer due to the velocity gradient across the glycocalyx and changes in the volume density of resistive segments. In the particle frame of reference the hydrodynamic shear plane determines the zero velocity location. In the calculations this was set at the bilayer to glycocalyx interface (0 Å). The volume density of segments is calculated from the surface density of segments and the length over which these are distributed. Two resistive elements, independent except for the common segment radius parameter, may be used. One (polymer I), associated with the glycocalyx, assumes a uniform distribution over the glycocalyx limits. The other (polymer II) assumes a uniform distribution over lower and upper limits freely set between 0 % and 120 % of the glycocalyx's depth. The latter was originally included to model adsorbed polymer but is used here to include the effect of different dimensions for tetra-EC and the glucuronic acid derivative of tetra-EC (tetra-ECG) when they are present in the same liposome preparation.

The surface density of segments is calculated from the surface

density of molecular species and the number of segments per molecule. The latter was calculated from molecular lengths and the assumed segment radius.

Fitting Results

The mobilities of three liposome preparations EL#3, EL#4 and EL#5 were fitted as functions of ionic strength. A fourth, EL#6, was intermediate in composition and behaviour to EL#4 and EL#5.

The EL#3 preparation was 50 % egg PC (PC), 10% DPPG (PG) and 40 % cholesterol. The model for the surface region has the charge at the bilayer-glycocalyx interface, i.e., inner charge at 0 Å. The combined surface density was 1.32×10^{14} molecules/cm^2. Phospholipid and cholesterol head group resistance was not considered initially but its effect was subsequently examined.

First, the charge density was varied while the head group resistance was held at zero (Fig. A4-1). Under this condition mobilities above 10 mM NaCl were best fit by a surface charge of 4500 esu/cm^2. This is much lower than the value calculated from the chemical composition of the lipid mixture from which the liposomes were formed, 10,700 esu/cm^2. Below 10 mM NaCl successively lower charge densities were required.

The head group resistance was then included (Figure A4-2) by allowing the PC and PG molecules to extend from the bilayer 8 Å, as estimated from the molecular structure. Two cases were considered. First, the number of segments per unit volume was varied in proportion to the depth. Thus the

segment volume density was held constant, implying that changing the length of the molecule changes the molecular mass. This does not coincide with experimental reality, however. Secondly, the segment volume density was held constant at the value used for the 8Å depth. In this case the segment volume density varies inversely with the extension, but the molecular mass is constant. This models a molecule which could collapse towards the surface, for instance. Comparison of the curves for the two case showed almost no difference over the length variation so in subsequent fitting only the constant molecular mass case was calculated.

The mobility was significantly reduced at all ionic strength by adding the head group resistance. The charge density had to be increased to 8,500 esu/cm^2 to match the high ionic strength data, a value near to that calculated from the assumed chemical composition.

The EL#4 preparation was 50 % PC, 10% PG, 10% cholesterol and 30% tetra-EC. The model for the surface region has the charge at 0 Å. The PC and PG parameters are as in preparation EL#3. The PEG chain on tetra-EC was estimated from molecular models to extend about 15 Å and the surface density was 6.6×10^{13} molecules/cm^2.

The data was fit by assuming β = 15 Å and varying the charge density (Figure A4-3). A value of 9,000 esu/cm^2, very close to that used to fit the bare PC/PG surface, fit the mobility value at 0.10 M. With the charge density constant β had to be varied to fit the points at the lower ionic strengths. The thicknesses had to be continuously increased to fit the data as lower ionic strength data was considered, the range being 15 to 73 Å.

A set of calculations was also carried out with both an 8 Å layer for the PC/PG head groups and a greater extension for the tetra-EC chains as described above. It was found that the resistance increase was small. A similar mobility fitting to that achieved above required the charge density to be increased to 9,500 esu/cm^2. However, the same range of thicknesses fit the data at lower ionic strengths when the charge density was held at 9,500 esu/cm^2.

The EL#5 preparation was 60 % PC, 10% cholesterol; 20% tetra-EC and 10% tetra-ECG. The model for the surface region has the charge at the outside of the glycocalyx adjacent to the free medium. The PC surface density is 1.32×10^{14} molecules/cm^2. The tetra-EC surface density was 4.4×10^{13} molecules/cm^2 and its extension taken to be 15 Å. The tetra-ECG head group was estimated to extend about 21 Å and the surface density was 2.2×10^{13} molecules/cm^2. The tetra-ECG surface charge density was varied (Figure A4-4) and found to fit the mobility in 0.10 M NaCl at 5,750 esu/cm^2 located at the extreme end of the molecule. The next two ionic strength points were likewise fit with this parameter set, but the two lowest values fell well above the line.

It is evident from the curves for other β values that the reduction in mobility with increase in molecular extension is much less in this instance than that obtained when the surface is modeled with all the charge at the base of the chains. The mobility is less sensitive to the chain extension when the charge is moved away from the the solid surface, presumably because the chains near the fixed charge plane offer less drag than the solid surface, at which the relative velocity must be zero.

The EL#6 preparation contained 25% tetra-EC and 5% tetra-ECG with 5% PG, 55% PC and 10% cholesterol. Hence, the overall chain density was as above but the charge was distributed half on the ends of the tetra-ECG chains and half at their base. In this case (Figure A4-5) an acceptable fit to the three highest ionic strength points was obtained if the charge values determined from best fits for EL#4 and EL#5 were each halved and assigned to the inner and outer charge layers in EL#6 and the polymer extensions taken as 15 Å and 21 Å for the tetra-EC and tetra-ECG chains respectively, demonstrating the consistency of the modeling at moderate ionic strengths.

Discussion

It is clear from the above results that the model of Sharp and Brooks can explain the general features of the effect on the electrophoretic mobility of adding neutral polymer chains to charged liposomes providing the data is not taken at ionic strengths below 10 mM. The values for the charge density agree reasonably well with those expected from the lipid composition provided the charge is located at the plane of the solid surface. In order to fit data obtained when the charge was located at the end of the chains on tetra-ECG the value was somewhat lower, however.

The inability of the theory to fit the data in any system at low ionic strength, in the presence or absence of surface-associated polymer chains, suggests that the charge density in fact varied as a function of ionic strength. This could reflect the binding of cations or impurities to the phosphate and acidic sugar moieties, a possibility that was not examined quantitatively. The fact that ß had to be increased as the ionic

strength was decreased when the charge was located at the base of the PEG chains could be interpreted to mean the chain extension increased in lower ionic strength media. This seems an unlikely explanation, however, as the chain is electrically neutral and and its configuration would not be expected to be very sensitive to ion concentration in the range examined here. It seems more likely the effect is associated with the relatively low values of mobility observed in low ionic strengths, the reason for which is not known.

Figure A4-1

LIPOSOME MOBILITY in pH 6.9 NaCl

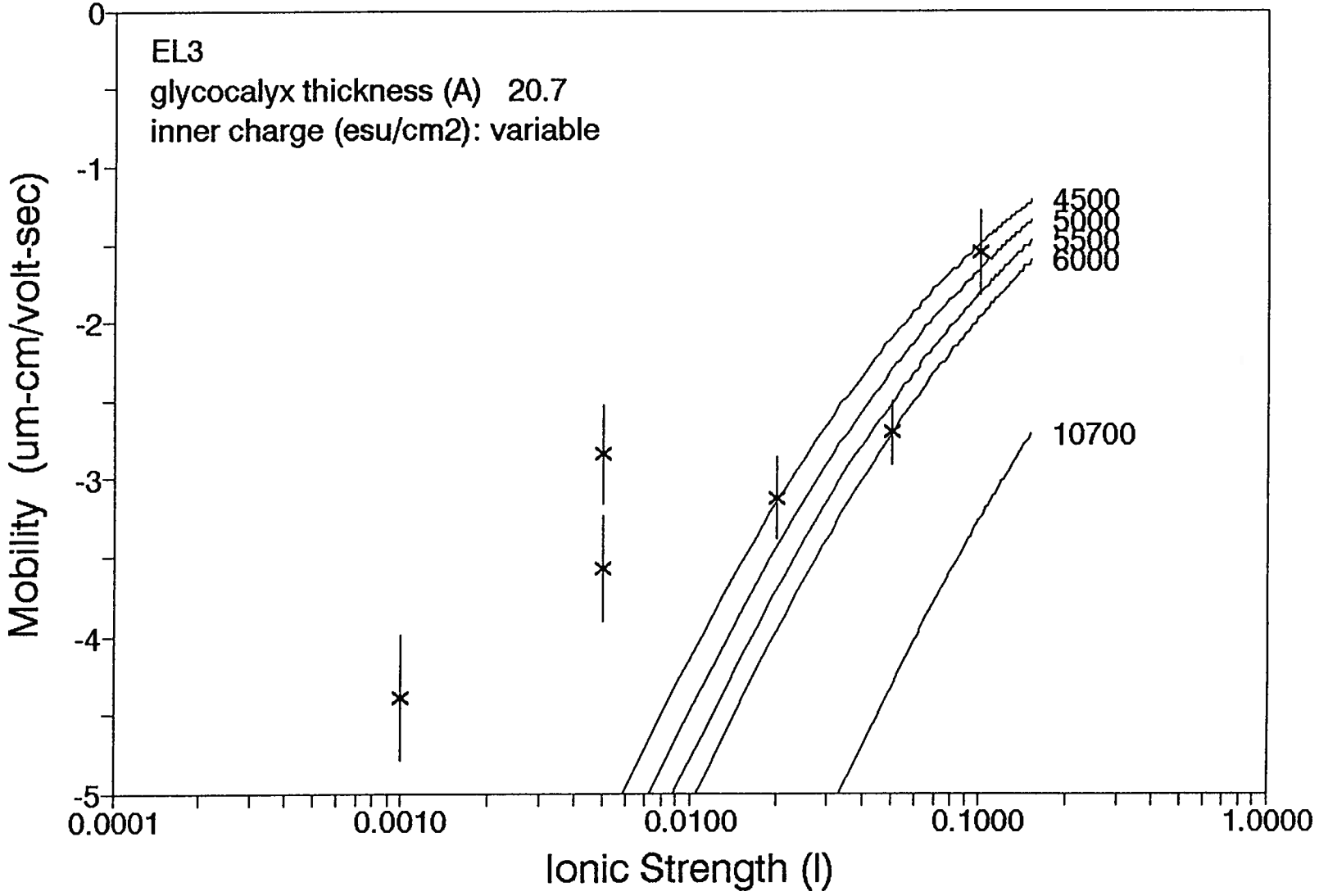

Figure A4-2

LIPOSOME MOBILITY in pH 6.9 NaCl

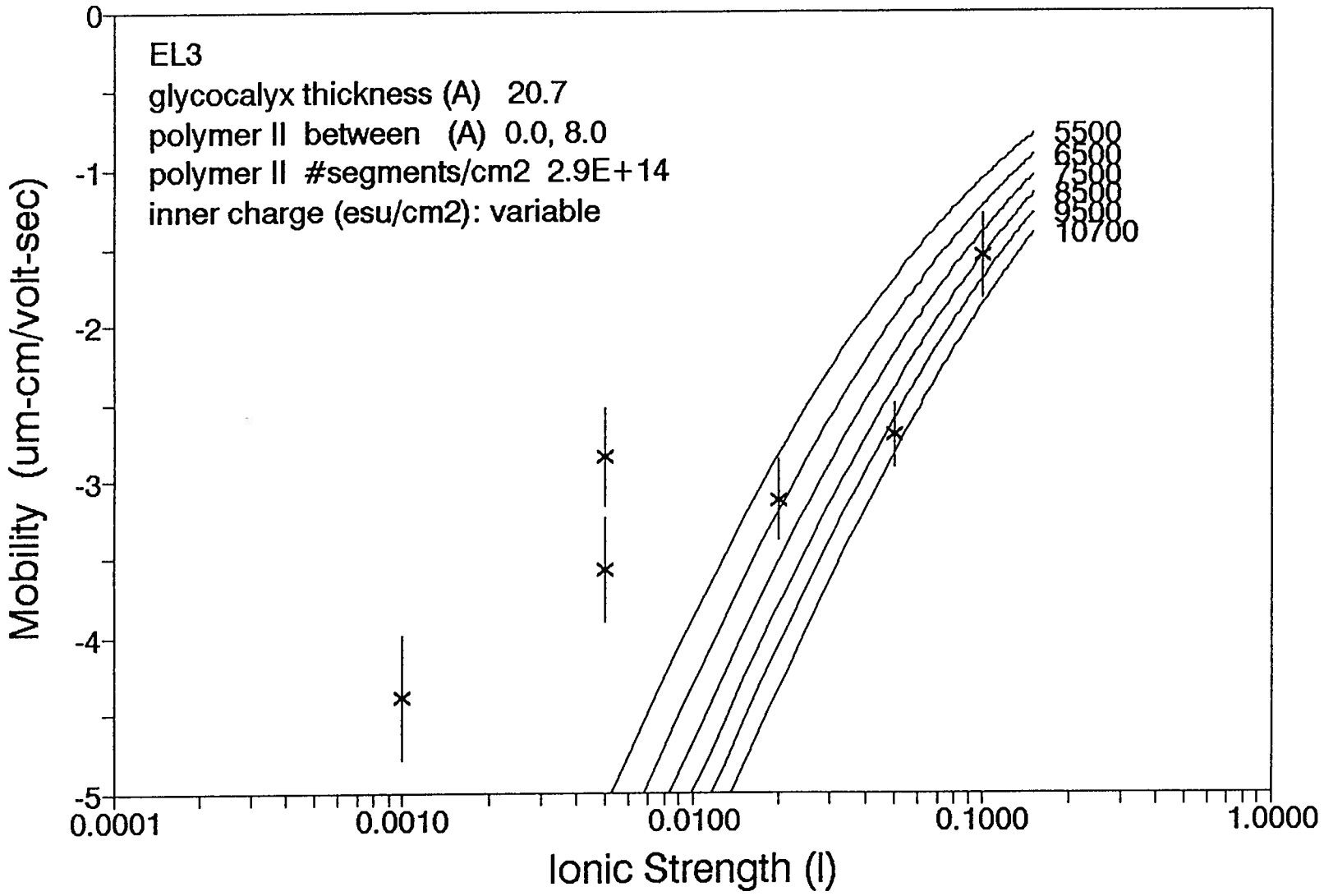

Figure A4-3

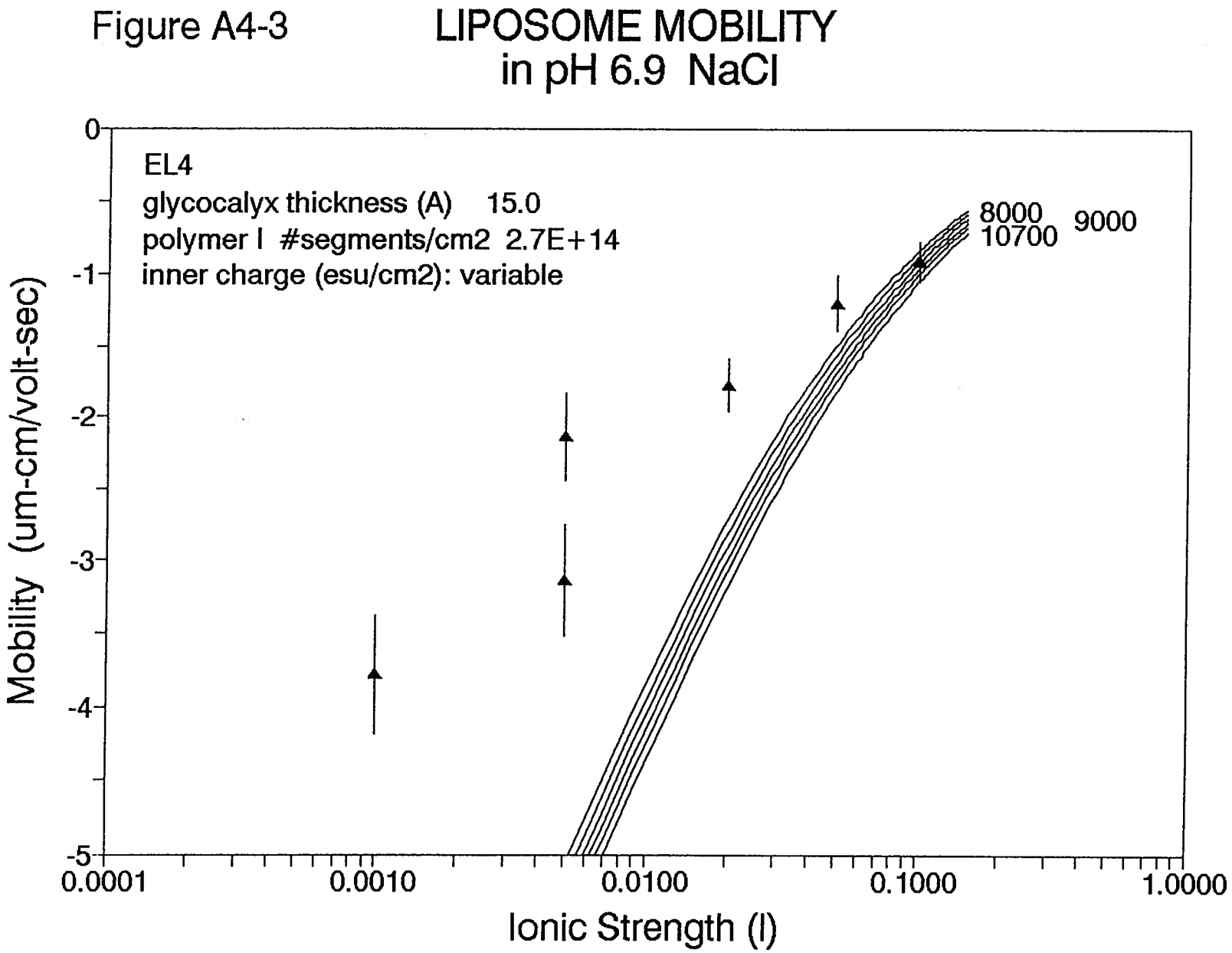
LIPOSOME MOBILITY
in pH 6.9 NaCl
EL4
glycocalyx thickness (A) 15.0
polymer I #segments/cm2 2.7E+14
inner charge (esu/cm2): variable
8000
9000
10700
Mobility (um-cm/volt-sec)
0
-1
-2
-3
-4
-5
0.0001
0.0010
0.0100
0.1000
1.0000
Ionic Strength (I)

Figure A4-4

LIPOSOME MOBILITY in pH 6.9 NaCl

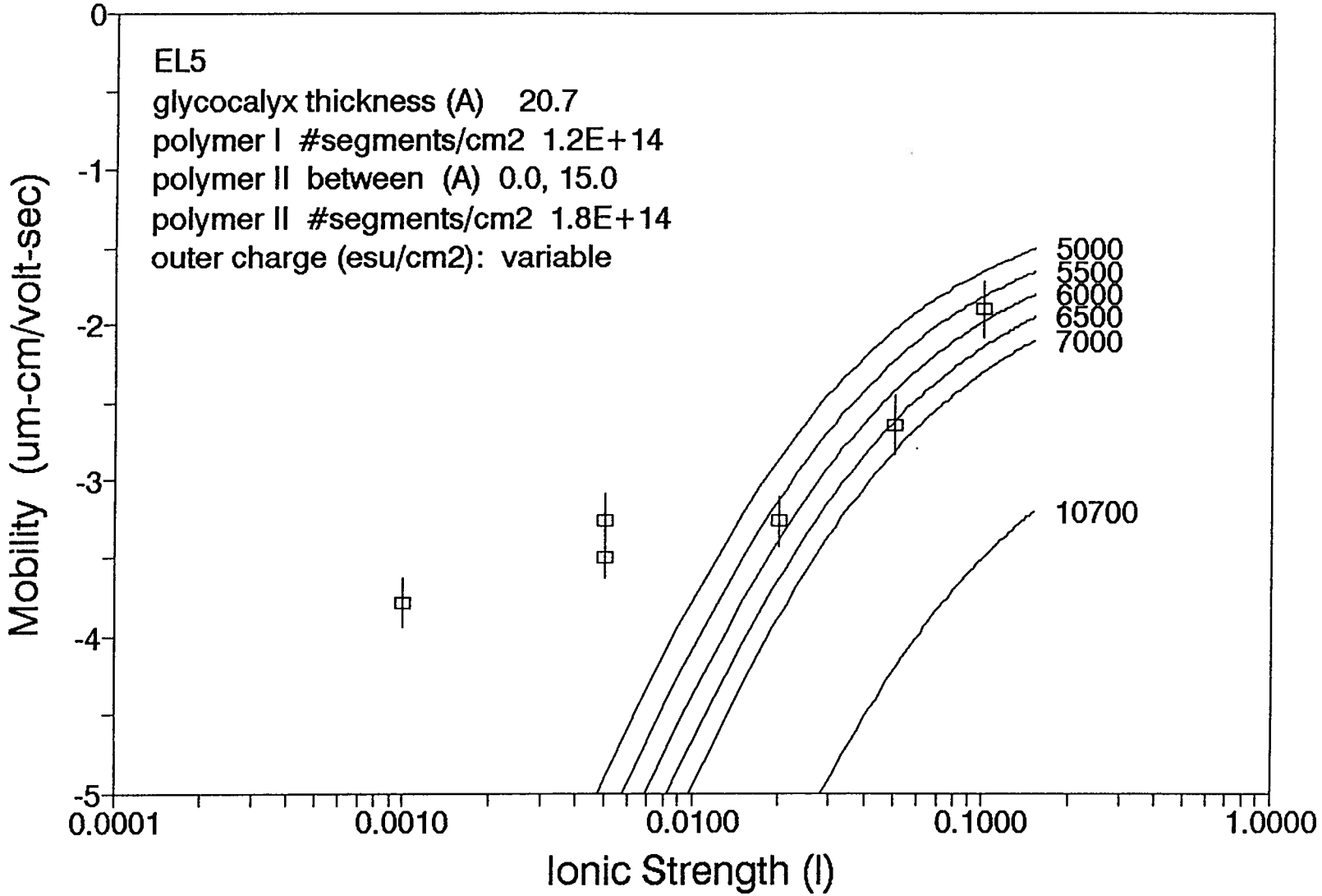

Figure A4-5

LIPOSOME MOBILITY in pH 6.9 NaCl